

Provenance and tectonic setting of the Early Permian sedimentary succession in the southern edge of the Sydney Basin, eastern Australia

Angelos G. Maravelis¹ | Robin Offler² | George Pantopoulos³ | William J. Collins⁴

¹Department of Geology, Aristotle University of Thessaloniki, Thessaloniki, Greece

²School of Environmental and Life Sciences, University of Newcastle, Callaghan, New South Wales, Australia

³Instituto de Geociências, Universidade Federal do Rio Grande do Sul (UFRGS), Porto Alegre, Brazil

⁴The Institute for Geoscience Research (TIGeR), Department of Applied Geology, Curtin University, Perth, Western Australia, Australia

Correspondence

Angelos G. Maravelis, Department of Geology, Aristotle University of Thessaloniki, 54124 Thessaloniki, Greece.

Email: angmar@geo.auth.gr

Funding information

NSW Institute for Frontiers Geoscience (IFG)

Handling Editor: J. S. Armstrong-Altrin

Early Permian basins formed during a major phase of crustal extension are common throughout eastern Gondwana. One of these basins, the Sydney Basin, has not been subjected to geochemical studies aimed at determining the sedimentary provenance and the tectonic setting. This study provides new geochemical data of the Lower Permian siliciclastic successions in the southern edge of the Sydney Basin. Published petrographic analysis indicates a source area containing sedimentary, felsic volcanic, plutonic, and low-grade metamorphic rocks. Major, trace and rare earth element data suggest that the clastic rocks are geochemically mature and originated from a continental source that has been subjected to moderate to strong weathering. Further, they indicate that most source rocks were of felsic composition and that only the oldest sediments possess a more mafic signature. The provenance data presented in this study, along with published palaeocurrent data, point to the Lachlan orogen being the main source of sediments for the basin. Multi-dimensional discrimination diagrams suggest a continental rift setting and agree with the published sequence stratigraphic framework that suggests a deepening-upward depositional trend associated with tectonic subsidence. This study documents geochemically the provenance of the sedimentary successions within the southern edge of the Sydney Basin and the continental rift origin of the basin.

KEY WORDS

Permian, provenance, rift basin, southern edge of the Sydney Basin, tectonic setting

1 | INTRODUCTION

Major, trace, and rare earth elements (REE) in sediments and sedimentary rocks have been applied to recent basin analysis studies for unravelling the geochemical signatures of the sedimentary successions (e.g., Armstrong-Altrin, 2009; Dimalanta et al., 2018; Maravelis, Pantopoulos, Tserolas, & Zelilidis, 2015; Pantopoulos & Zelilidis, 2012). Several geochemical discrimination diagrams have been proposed to determine the provenance and tectonic setting of sedimentary basins (e.g., Bhatia, 1983; Condie, Noll Jr, & Conway, 1992; McLennan, Taylor, McCulloch, & Maynard, 1990; Roser & Korsch, 1986; Verma & Armstrong-Altrin, 2013). Earlier studies had

limitations because the diagrams proposed by Bhatia (1983) and Roser and Korsch (1986) could not discriminate sediments from different geotectonic settings (e.g., collisional and continental rift settings). Further, the statistical methods used in the construction of these diagrams have been questioned because they often lead to incorrect interpretations of the tectonic setting (Verma & Armstrong-Altrin, 2013, 2016). Therefore, the discriminant function (DF) multi-dimensional diagrams proposed by Verma and Armstrong-Altrin (2013, 2016) have been utilized in recent studies (Nagarajan et al., 2015; Offler & Fergusson, 2016; Tawfik et al., 2017). These diagrams are preferable since they have been constructed considering the influence of analytical errors, source weathering, sediment recycling, and

diagenesis on the major element abundances. The application of these diagrams using data from well-constrained tectonic settings has been proven valuable, and in agreement with settings based on other geological data.

The Lower Permian sedimentary succession in the southern edge of the Sydney Basin (referred to henceforth as SSB), eastern Australia, offers an opportunity to better constrain the provenance and regional tectonic setting from the geochemistry of the sedimentary rocks. Further, the SSB offers a framework for understanding the nature and intensity of extension-related processes that controlled the accommodation and stratigraphic architecture of the SSB in eastern Gondwana during the Early Permian. The study area containing this succession is located SSW of Sydney, Australia (Figure 1). The Sydney Basin is economically significant because it is a well-established coal-producing

province and exhibits hydrocarbon generation potential (e.g., Alder et al., 1998; Hutton, 2009; Maravelis, Chamaki, Pasadakis, Zelilidis, & Collins, 2017). It is compiled by a complex system of depocentres that form the southern margin of the larger, N-S trending Bowen-Gunnedah-Sydney Basin (Glen, 2005).

This study is focused on the onshore sector of the SSB that contains the Lower Permian clastic rocks belonging to the Wasp Head (~100 m thick, Early to Middle Sakmarian, based on palaeontological studies of Runnegar, 1980), Pebbley Beach (~150 m thick, Sakmarian to Artinskian, based on palaeontological studies of Briggs, 1998), and Snapper Point (300–400 m thick, Early Kungurian, based on palaeontological studies of Veevers, Conaghan, & Powell, 1994) formations (Eyles, Eyles, & Gostin, 1998; Fielding, Bann, MacEachern, Tye, & Jones, 2006; Gostin & Herbert, 1973; Rygel et al., 2008; Tye,

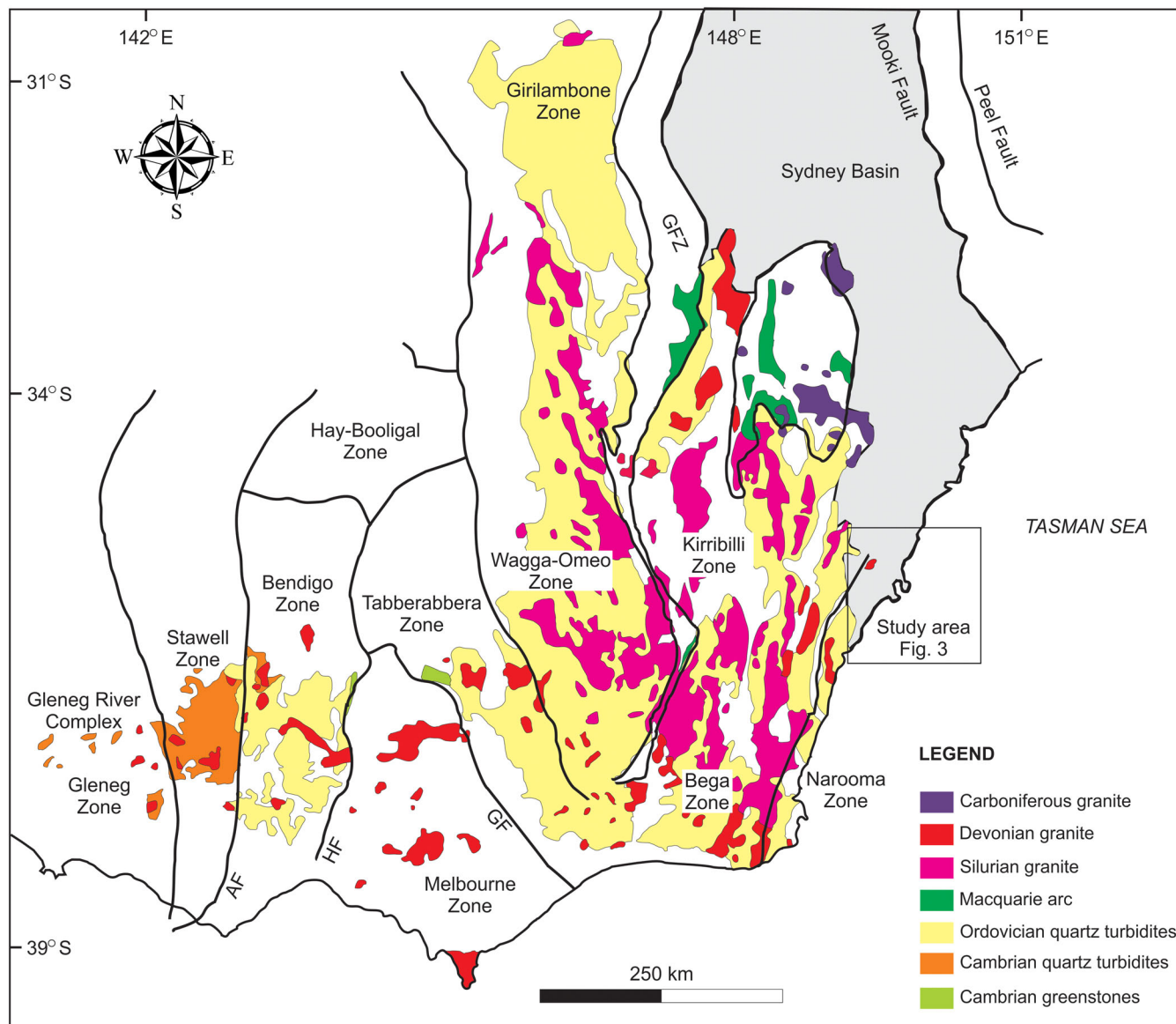


FIGURE 1 Geological map of Lachlan orogen and surrounding regions depicting the distribution of Ordovician turbidites (Adaminaby Group and equivalents) and volcanic and volcanoclastic rocks. AF, Avoca Fault; GF, Governor Fault; GFZ, Gilmore Fault Zone; HF, Heathcote Fault Zone (modified from Glen, 2013) [Colour figure can be viewed at wileyonlinelibrary.com]

Fielding, & Jones, 1996). Recently, it has been proposed that the uppermost parts of the Pebbley Beach Formation belong to a different formation (Mount Agony Formation, 15–20 m thick), based on sedimentological and sequence stratigraphic analysis (see Maravelis, Catuneanu, Nordsvan, Landenberger, & Zelilidis, 2018 and Rygel et al., 2008 for extensive discussions). Detailed sedimentological, stratigraphic, and petrographic investigations have been carried out by Eyles et al. (1998); Fielding et al. (2006); Gostin and Herbert (1973); Maravelis et al. (2018); Rygel et al. (2008); and Tye et al. (1996). However, studies on the provenance and tectonic setting of the sediments that filled the SSB based on their geochemistry are lacking.

In view of the absence of such data, chemical analyses of sandstone and mudstone samples have been carried out. Because most major elements (e.g., K, Na, Ca) are mobile during weathering and diagenesis (Dostal & Keppie, 2009), the determination of provenance and tectonic setting is mainly based on immobile elements (e.g., Zr, Y, Th, Ti, and REE, McLennan, 1989). The objectives of this study are to determine the geochemical signature of the Lower Permian siliciclastics within the SSB and reveal their provenance and geological setting.

2 | TECTONO-STRATIGRAPHIC SETTING

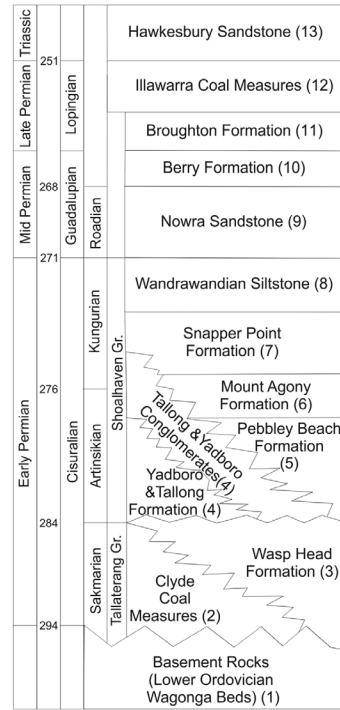
During the Permian–Early Triassic, Australia was part of the active continental margin of eastern Gondwana (Veevers et al., 2006). In the

Early to Middle Permian, subduction retreat led to extension of the pre-existing Carboniferous continental volcanic arc, resulting in the formation of a series of rift basins including the Sydney Basin (e.g., Jenkins, Landenberger, & Collins, 2002; Korsch, Totterdell, Catbro, & Nicoll, 2009; Shaanan, Rosenbaum, & Wormald, 2015). In this geodynamic framework, the Sydney Basin was formed as an inboard, continental Early Permian rift basin, which is underlain by the Lachlan orogen to the south and the New England orogen to the north (Eyles et al., 1998; Gostin & Herbert, 1973; Figure 1) and constitute parts of the larger-scale Terra Australis orogen (Cawood, 2005).

The Early Permian stratigraphic evolution of the SSB is illustrated in Figure 2. During the initial rifting stage, the sediments of the Wasp Head Formation and Clyde Coal Measures were accumulated unconformably on the basement (Ordovician Wagonga Beds) that is composed of deformed and metamorphosed rocks of the Lachlan orogen (Gostin & Herbert, 1973). The Wasp Head Formation is composed of breccias and sandstone beds, with the clasts in the breccias consisting of phyllite and chert in a lithic sandstone to mudstone matrix (Gostin & Herbert, 1973). The Wasp Head Formation has been considered as either fluvial (Maravelis et al., 2018) or marine (Rygel et al., 2008) in origin, whereas the Clyde Coal Measures are interpreted as terrestrial deposits (Tye et al., 1996). The overlying Pebbley Beach, Mount Agony, and Snapper Point formations correspond to marginal marine and fully marine environments of deposition (Fielding et al., 2006; Maravelis et al., 2018). They reflect deposition during a later episode of more uniform, regional subsidence (Fielding

SOUTHERN SYDNEY BASIN

Maravelis et al., (2018)



Fielding et al., (2006)

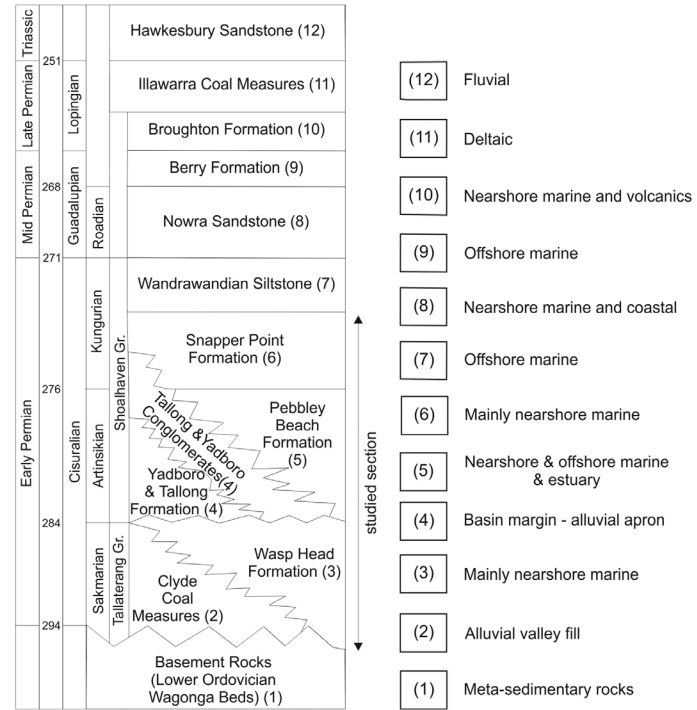


FIGURE 2 Comparable litho-stratigraphy of the southern edge of the Sydney Basin, as proposed by Fielding et al. (2006) and Maravelis et al. (2018)

et al., 2006). The tephra that occurs in the overlying Wandrawandian siltstone suggests that subduction related calc-alkaline continental arc volcanism existed along the margin of the New England orogen (Herbert & Helby, 1980). These sediments represent an outer shelf

depositional environment (Thomas, Fielding, & Frank, 2007) that was developed during a period of high relative sea level and increased subsidence (Eyles et al., 1998). The overlying Nowra Sandstone is regarded as shoreface (Eyles et al., 1998) and fluvial (Le Roux &

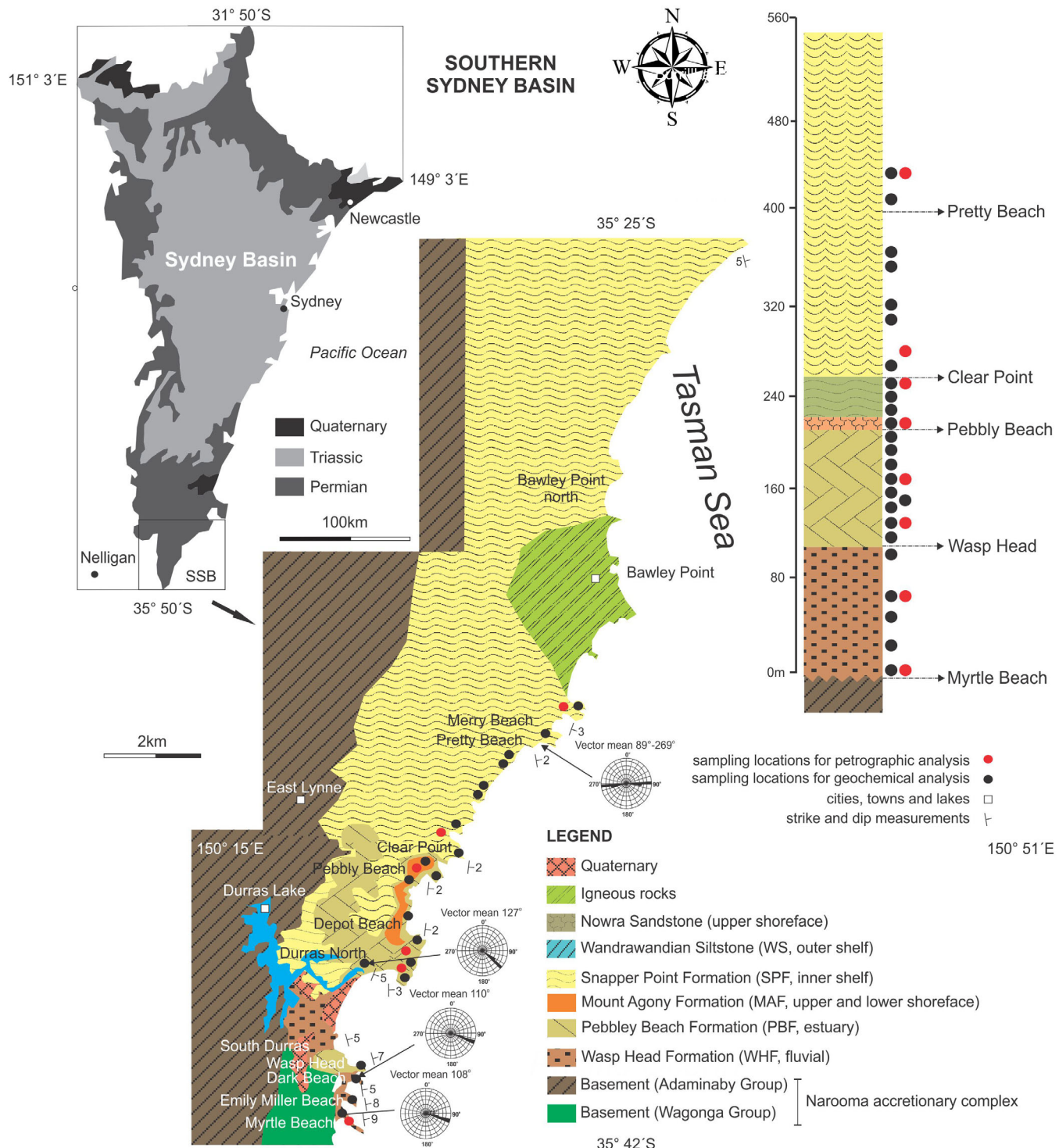


FIGURE 3 Geological map of the southern Sydney Basin depicting the up-sequence evolution during the Early to Middle-Permian (modified from Eyles et al., 1998; Fielding et al., 2006; Maravelis et al., 2018; Tye et al., 1996). The black dots correspond to the studied locations for geochemical analysis and the red dots correspond to the studied locations for petrographic analysis. Palaeodispersal data are from Fielding et al. (2006) and Rygel et al. (2008) [Colour figure can be viewed at wileyonlinelibrary.com]

Jones, 1994) deposits, and the overlaying Berry Siltstone reflects the basin-scale transgression and deposition in an offshore depositional environment (Eyles et al., 1998).

The Middle Permian to Middle to Late Triassic Hunter–Bowen orogeny was responsible for the change of the Sydney Basin to a foreland basin (e.g., Collins, 1991; Holcombe et al., 1997). The deformation related to this orogeny displays spatial and temporal variations and is characterized by shorter and regional deformational cycles that occurred within the longer Gondwanide orogeny (Hoy & Rosenbaum, 2017). The Hunter–Bowen orogeny is the result of plate coupling, related to changes in global plate configuration and increased convergence rates (Hoy & Rosenbaum, 2017; Rosenbaum, 2018). Furthermore, local differentiations in parameters, such as flatness of the subduction zone or, less likely, terrane accretion could have played an additional role (Catuneanu, Hancox, Cairncross, & Rubidge, 2002; Rosenbaum, 2018).

The deformation associated with the Hunter–Bowen orogeny during the Middle–Late Triassic was related to along-strike variations in the amount of coupling across the subduction zone (Hoy & Rosenbaum, 2017). The Middle and Late Triassic tectonic setting is represented by folding and uplift during the last stage of Hunter–Bowen orogeny (Babaahmadi, Sliwa, Esterle, & Rosenbaum, 2017; Campbell, Shaanan, & Verdel, 2017). This deformation led to west directed thrust faults and reactivation of normal faults (Korsch et al., 2009).

3 | MATERIALS AND METHODS

Twenty sandstone and five mudstone samples were collected from the four formations for geochemical analyses (Figures 3 and 4). Additionally, eight fine- to medium-grained, samples of sandstone were collected for petrographic analysis (Figures 3 and 4). The samples were ground to powders in a tungsten-carbide mill. All analyses were performed on fused discs made from the rock powders. Major, trace, and REE abundances were determined by Intertek Genalysis Laboratory Services using ICP-OES (major elements) and ICP-MS (trace elements and REE) respectively; loss on ignition (LOI) was determined from 1 g of sample heated at 1,050°C. Geochemical studies of sedimentary rocks that have been deposited in an inferred tectonic setting are recalculated dry to secure suitability for comparison with modern, known tectonic settings (Rollinson, 1993). Thus, for statistical coherency, the use of major element contents in various plots was performed after recalculation to an anhydrous (LOI-free) basis and adjustment to 100%. Major, trace, and REE contents of the SSB samples are presented in the geochemistry supplementary data document (Table S1). The sandstone samples were petrographically analysed using a Zeiss Axio plan Research microscope. Characteristics such as grain shape, types of mineral present, and types of rock fragments were utilized to define the detrital assemblages in the formations and reveal their provenance. The observations made in these analyses were compared with those made by Gostin (1968) in a previous detailed study.

Multivariate major, trace, and REE compositional datasets were processed via principal component analysis (PCA) using R software (R Core Team, 2020). This statistical technique has been used in sedimentary provenance studies for grouping of samples based on multivariate compositional (bulk geochemical or petrographic) datasets. The reader is referred to von Eynatten, Barceló-Vidal, and Pawlowsky-Glahn (2003) and Nielsen, Weibel, and Friis (2015) for analytical descriptions and references regarding the PCA method. Discrimination of tectonic setting for the studied sedimentary rocks was performed using the discriminant-function-based multi-dimensional diagrams proposed by Verma and Armstrong-Altrin (2013, 2016). In these diagrams, the dataset is analysed using the isometric log-ratio transformation (ilr) technique (Egozcue, Pawlowsky-Glahn, Mateu-Figueras, & Barceló-Vidal, 2003). The samples with MnO content below detection limit were not plotted because the DFs of Verma and Armstrong-Altrin (2013) have a natural logarithm (Ln) normalization resulting in samples with MnO content of 0% producing unsatisfactory results (the samples plot in geologically unreasonable fields, over the diagram).

4 | RESULTS

4.1 | Petrography

Because detailed petrographic analyses of the sedimentary rocks in the study area have been carried out by Gostin (1968), this study offers a brief summary of the main features of samples collected in different formations. Sandstone from the Wasp Head, Pebbley Beach, Mount Agony, and Snapper Point formations are dominantly well-sorted, even, very fine- to medium-grained, arenites containing angular to sub-angular, mono-, and polycrystalline quartz, and lithic clasts (Table S2). Gostin (1968) documented a marked change in the composition of the sandstone beds from the Wasp Head Formation, compared with all the other formations. The sandstone in the lower Wasp Head Formation is lithic arenite, whereas those in the upper part and within the other formations are feldspatho-lithic, litho-feldspathic, and sub-labile arenites (*sensu* Crook, 1960) with similar proportions of feldspar and rock fragments (Figure 5). It needs to be stressed that the Wasp Head and Mount Agony formations, as defined by the present study, correspond to the lower part of Wasp Head Formation and upper part of Pebbley Beach Formation of Gostin (1968). Quartz often exhibits undulose extinction. Less common are plagioclase and muscovite, and uncommon are opaque minerals and perthitic K-feldspar (Figure 6). The latter is only present in Snapper Point and Pebbley Beach formations. Subhedral to sub-rounded zircon and tourmaline are accessory minerals. Rare hornblende, biotite, and composite grains made up of quartz-K-feldspar, quartz-plagioclase, and graphic intergrowths of quartz-feldspar also occur. Lithic clasts dominate some samples and include sedimentary, felsic volcanic, and low-grade metamorphic rocks such as chert, siliceous, radiolarian-bearing lutite, siltstone, meta-siltstone, slate, and quartzite (Figure 6). Several clasts are extensively replaced by fine-grained aggregates of white

mica (illite). Gostin (1968) reported a prominent change in the types of lithic clasts that occur in the Wasp Head Formation, compared with the clasts within all the other formations. The lower part of the Wasp Head Formation (entire Wasp Head Formation as defined in this study) is dominated by low-grade metamorphics (argillite, chert, and quartzite), with lesser contribution of volcanic rock fragments. In contrast, the upper part of the Wasp Head Formation and the other

formations are composed of volcanic rock fragments, at the expense of low-grade metamorphics. The detrital components in all formations are generally similar; however, biotite and K-feldspar were not observed in the Wasp Head Formation. Matrix is represented by minerals, such as siderite, fine-grained white mica (illite), calcite, and less commonly quartz and semi-opaque aggregates that fill the pore spaces between detrital grains.

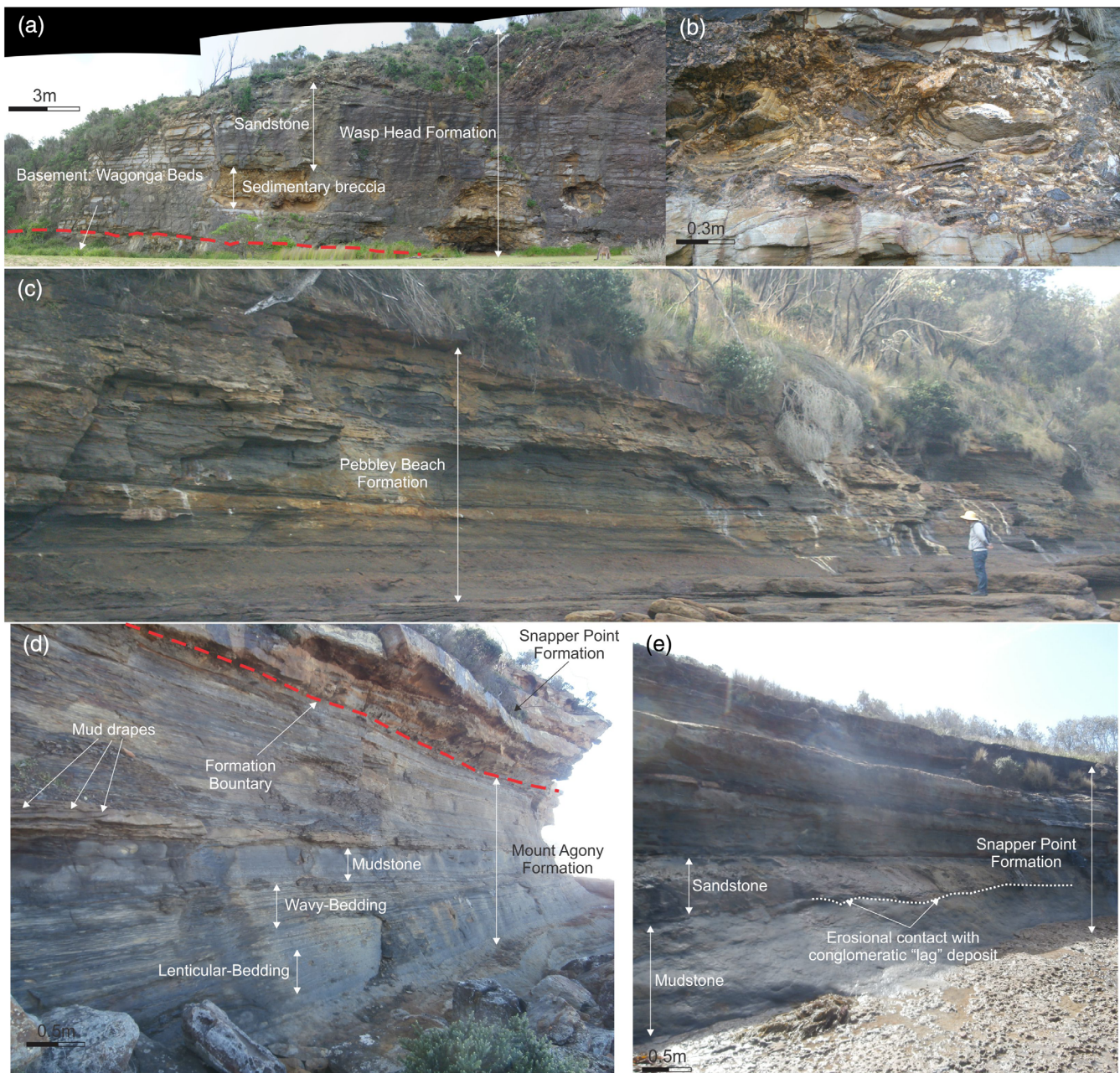


FIGURE 4 Outcrop photographs illustrating diagnostic features of the Lower Permian sediments in the southern Sydney Basin. (a) Repetitions of coarse-grained sandstone and conglomerate (Myrtle Beach, Wasp Head Formation). Note the fining-upward trend that suggests progressive decrease in fluvial energy with time. (b) Close-up view of the Wasp Head Formation illustrating the presence of angular and very angular clasts in the brecciated deposits. (c) Thin- to thick-bedded, marginal marine (estuarine system) sandstone interbedded with mudstone (Pebbley Beach, Pebbley Beach Formation). (d) Sheet-like lenticular and flaser-bedded sandstone beds, intercalated with cross-bedded sandstone and overlying mud drapes (Clear Point, Mount Agony Formation). (e) Thin- to thick-bedded, shallow marine (inner shelf) sandstone interbedded with mudstone (Clear Point, Snapper Point Formation). Person for scale is 180 cm tall [Colour figure can be viewed at wileyonlinelibrary.com]

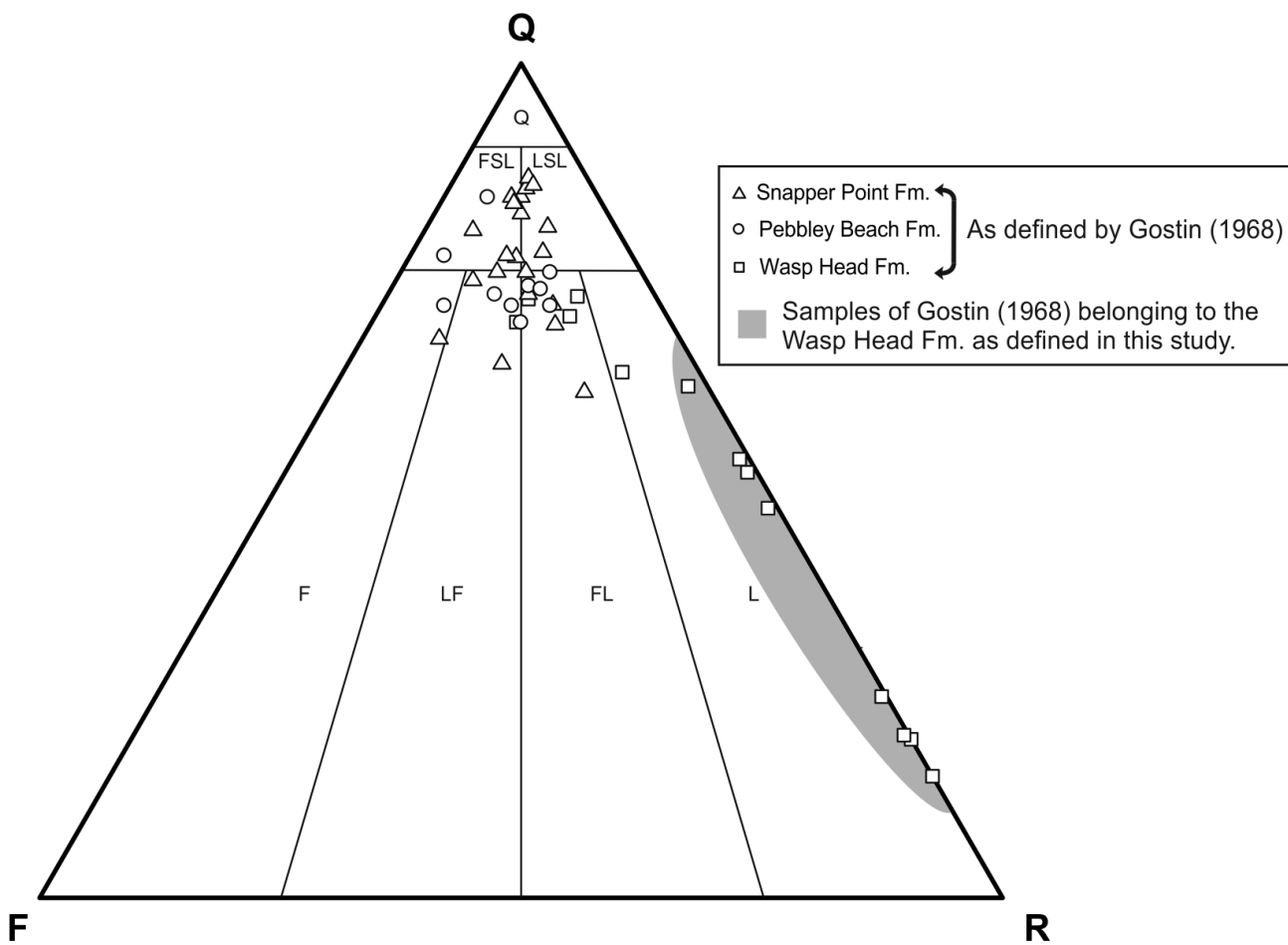


FIGURE 5 QFR (quartz, feldspar, rock fragments) ternary diagram of Crook (1960) based on thin section point-counting data from Gostin (1968). Shaded area covers samples that belong to the Wasp Head Formation as defined by the present study (lower half of Wasp Head Formation of Gostin, 1968). F, feldspathic arenite; FL, feldspatho-lithic arenite; FSL, feldspathic sub-labile arenite; L, lithic arenite; LF, litho-feldspathic arenite; LSL, lithic sub-labile arenite; Q, quartzose arenite

4.2 | Major element abundances

The mean SiO_2 contents range from 77.81 wt% in the Wasp Head Formation to 62.93 wt% in the Mount Agony Formation. Wasp Head Formation is enriched in SiO_2 relative to the Upper Continental Crust (UCC, 66.62 wt%, Rudnick & Gao, 2003), in contrast to the Pebbley Beach, Mount Agony, and Snapper Point formations that possess similar SiO_2 contents to the UCC. The mean Al_2O_3 content is between 11.43 wt% in the Wasp Head Formation and 16.16 wt% in the Mount Agony Formation. In most formations (except Mount Agony Formation), the mean Al_2O_3 content is slightly lower than that of the UCC (15.4 wt%). The mean Fe_2O_3 content varies from 1.85 wt% in the Wasp Head Formation to 9.53 wt% in the Snapper Point Formation. The average K_2O contents range from 1.85 to 3.24 wt% in the Wasp Head Formation and Mount Agony Formation, respectively, and Na_2O is between 0.81 and 1.25 wt% (in the Mount Agony Formation and Wasp Head Formation, respectively). The contents of MnO and P_2O_5 are very low and display no major differences between the different

formations. LOI values range from 3.61 to 15.98 wt% (Table S1). The types of minerals that occur in sedimentary rocks control the distribution of major and trace elements, and Pearson's correlations of Al_2O_3 versus SiO_2 , TiO_2 , and K_2O (Figure 7) are used to evaluate their effect on major element abundances in the studied formations (Bauluz, Mayayo, Fernandez-Nieto, & Gonzalez Lopez, 2000). In the SSB samples, SiO_2 exhibits strong negative correlation with Al_2O_3 (Figure 7) for all studied formations except Snapper Point Formation. In contrast, positive linear correlations exist between K_2O and TiO_2 with Al_2O_3 (Figure 7). All samples display $\text{K}_2\text{O}/\text{Al}_2\text{O}_3$ ratios below 0.3.

Based on their logarithmic ratios of $\text{SiO}_2/\text{Al}_2\text{O}_3$ versus $\text{Fe}_2\text{O}_3/\text{K}_2\text{O}$ (Herron, 1988), the sandstone and mudstone samples are classified as shales, wackes, litharenites, and arkoses (Figure 8). The samples that belong to Pebbley Beach, Mount Agony, and Snapper Point formations are chiefly classified as wackes, whereas arkoses represent the principal rock type of samples from the Wasp Head Formation. One mudstone sample from Snapper Point Formation was classified as Fe-shale (Figure 8).

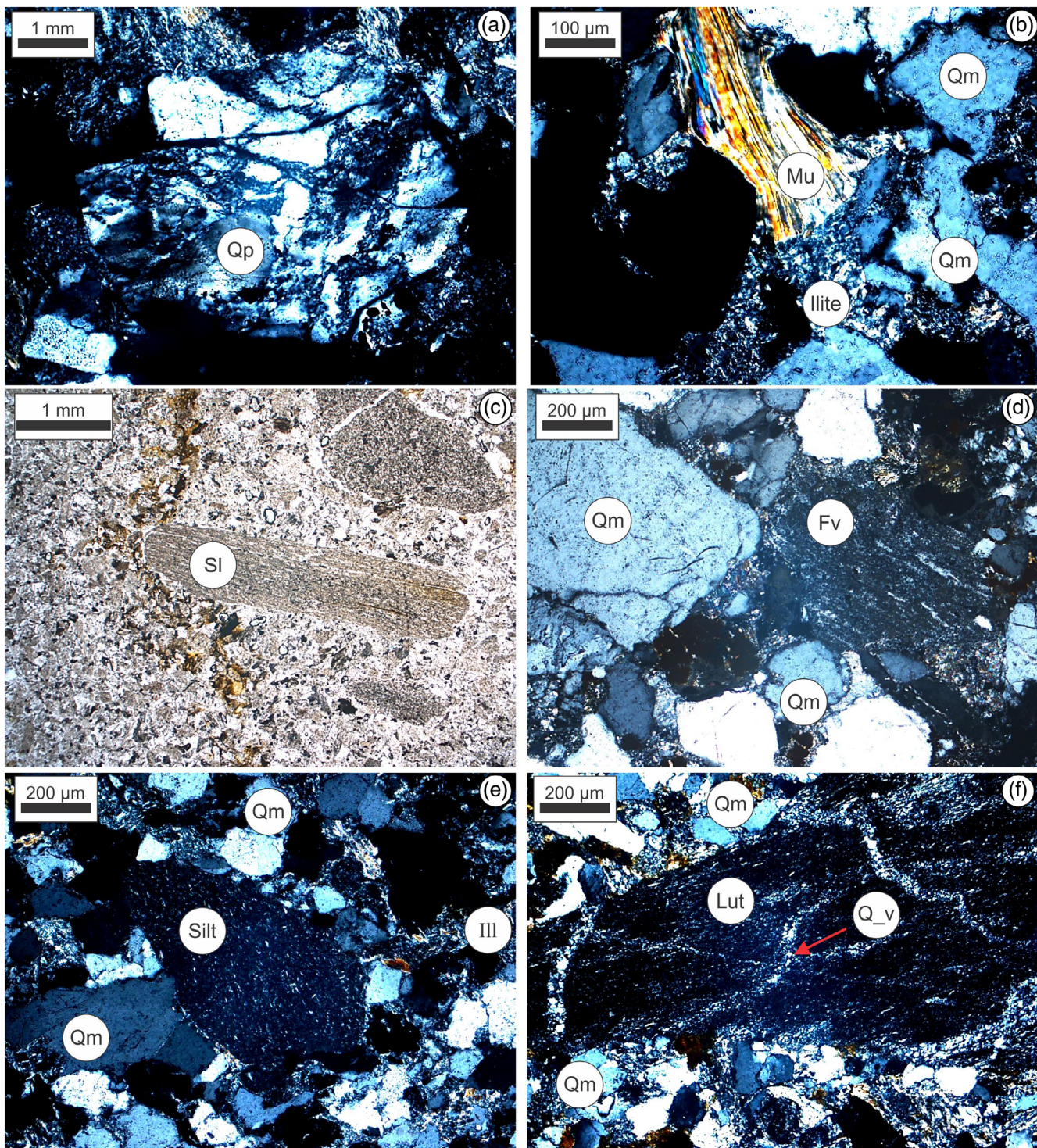


FIGURE 6 Photomicrographs illustrating features of the sandstones from the Lower Permian studied formations in the southern Sydney Basin. (a) Polycrystalline quartz showing dynamic recrystallization, fracturing, and undulose extinction in parts of grain (Wasp Head Formation). (b) Detrital muscovite and monocrystalline quartz. Note illite and quartz in pore space (Snapper Point Formation). (c) Slate clast (centre, Wasp Head Formation, uncrossed Nicols). (d) Layering in felsic volcanic clast (Pebbley Beach Formation). (e) Siltstone clast. Monocrystalline quartz and fine-grained illite occurs in pore space (Snapper Point Formation). (f) Siliceous lutite containing folded quartz veins (Wasp Head Formation). Fv, felsic volcanic; III, illite; Lut, siliceous lutite; Mu, muscovite; Qm, monocrystalline quartz; Qp, polycrystalline quartz; Q_v, quartz veins; Sl, slate [Colour figure can be viewed at wileyonlinelibrary.com]

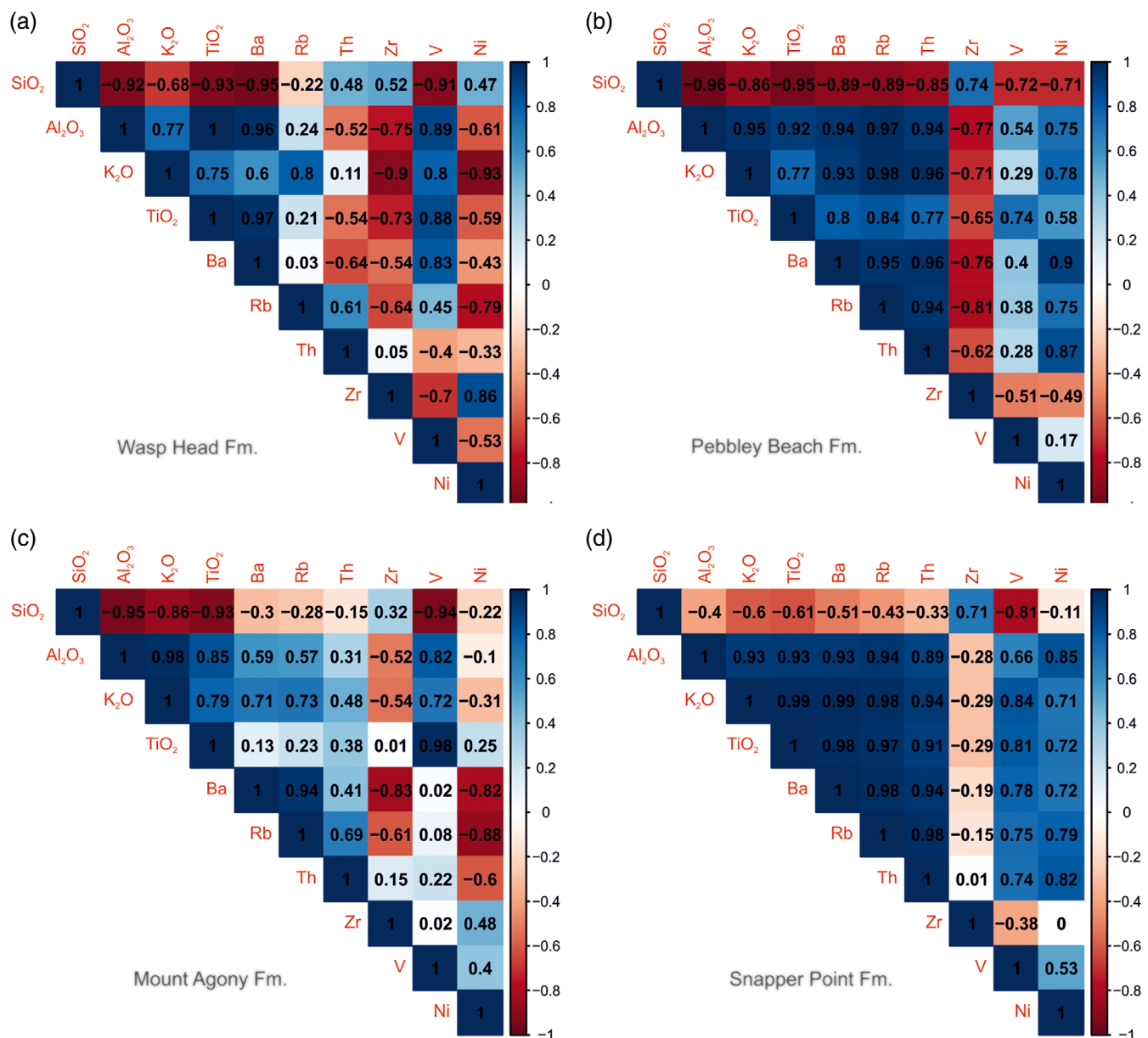


FIGURE 7 Pearson's r correlations for selected major element (SiO_2 , TiO_2 , K_2O , Al_2O_3) and trace element (Ba, Rb, Th, V, Ni, Zr) abundances for the studied southern Sydney Basin formations samples. (a) Wasp Head Formation, (b) Pebbley Beach Formation, (c) Mount Agony Formation, and (d) Snapper Point Formation [Colour figure can be viewed at wileyonlinelibrary.com]

4.3 | Trace element abundances

In order to determine the degree of enrichment or depletion of each trace element, with respect to the Post-Archean Australian Shale (PAAS) and evaluate the provenance of the studied sandstone and mudstone samples, the trace element values were normalized against PAAS (Figure 9). The large-ion lithophile trace elements (LILE) such as, Rb, Ba, Sr, Th, and U vary considerably. The Wasp Head Formation is enriched in Ba and U but depleted in Rb and Th relative to PAAS. Moreover, it displays slightly lower abundances of Zr and Hf compared to PAAS, but is enriched in Y and depleted in Nb. In contrast, Pebbley Beach, Mount Agony, and Snapper Point formations display

similar concentrations of Rb, Ba, Th, and U compared to PAAS; however, they are moderately depleted in Sr. They also display similar concentrations of Y and Zr compared to PAAS, but are slightly richer in Hf (Figure 9).

Pearson's correlations of trace elements versus Al_2O_3 indicate that Ba and Rb correlate positively with Al_2O_3 , especially in the Pebbley Beach and Snapper Point formations (Figure 7b,d). However, the correlation of Rb with Al_2O_3 is poor in the Wasp Head Formation. Similar correlations exist for Th and Al_2O_3 in the Pebbley Beach and Snapper Point formations (Figure 7b,d), but this correlation is not apparent in the Wasp Head and Mount Agony formations. Further, the samples lack statistically significant correlation between SiO_2 and

Zr for Wasp Head and Mount Agony formations (Figure 7a,c). Among transition trace elements (Cr, Co, Ni, V, and Cu), the samples from all formations are slightly enriched in Cr and V and are depleted in Ni. In contrast to the other formations, Wasp Head Formation is poorer in Co. Generally, Co, V, and Ni exhibit a poor correlation. The most important correlations exist between Al_2O_3 -V in Wasp Head and Mount Agony formations, and Al_2O_3 -Ni in Snapper Point Formation (Figure 7).

4.4 | Rare earth element abundances

The total REE content of samples ranges from 113.9 to 222.9 ppm for Wasp Head Formation, 123.7 to 261.8 ppm for Pebbley Beach Formation, 189.5 to 222.3 ppm for Mount Agony Formation, and 125.3 to 267.8 ppm for Snapper Point Formation (Table S1). The ratio between the light REE (LREE, La, Ce, Pr, Nd, Sm, and Eu) and heavy

REE (HREE, Gd, Tb, Dy, Ho, Er, Tm, Yb, Lu, and Y) ratio is high and variable amongst the different formations (Table S1). It is considerably higher in Pebbley Beach, Mount Agony, and Snapper Point formations ($\text{LREE}/\text{HREE} = 9, 8.3$, and 9.4) than in Wasp Head Formation (5.8). Overall, the chondrite-normalized REE patterns show moderate enrichment in LREE and relatively flat HREE patterns (Figure 10). The average $\text{La}_{\text{N}}/\text{Yb}_{\text{N}}$ and $\text{La}_{\text{N}}/\text{Sm}_{\text{N}}$ ratios (subscript N refers to chondrite-normalized values) are higher in Pebbley Beach, Mount Agony, and Snapper Point formations ($\text{La}_{\text{N}}/\text{Yb}_{\text{N}} = 9.01, 8.41$ and 9.11 , and $\text{La}_{\text{N}}/\text{Sm}_{\text{N}} = 3.87, 3.77$, and 3.74 , respectively) than in Wasp Head Formation ($\text{La}_{\text{N}}/\text{Yb}_{\text{N}} = 5.89$ and $\text{La}_{\text{N}}/\text{Sm}_{\text{N}} = 2.06$), indicating that the latter displays a less fractionated REE pattern. Furthermore, it exhibits less flat HREE segments (mean $\text{Gd}_{\text{N}}/\text{Yb}_{\text{N}} = 2.02$), in contrast to the other formations (mean $\text{Gd}_{\text{N}}/\text{Yb}_{\text{N}} = 1.42, 1.42$, and 1.45 , respectively). All samples display a negative Eu anomaly, but the average Eu/Eu^* [$([\text{Eu}/\text{Eu}^* = (\text{Eu})_{\text{N}}/([\text{Sm}]_{\text{N}} \times (\text{Gd})_{\text{N}})^{1/2})]$] in the Wasp Head Formation is higher (0.77) than in the Pebbley Beach, Mount Agony, and Snapper Point formations ($0.6, 0.59$, and 0.63).

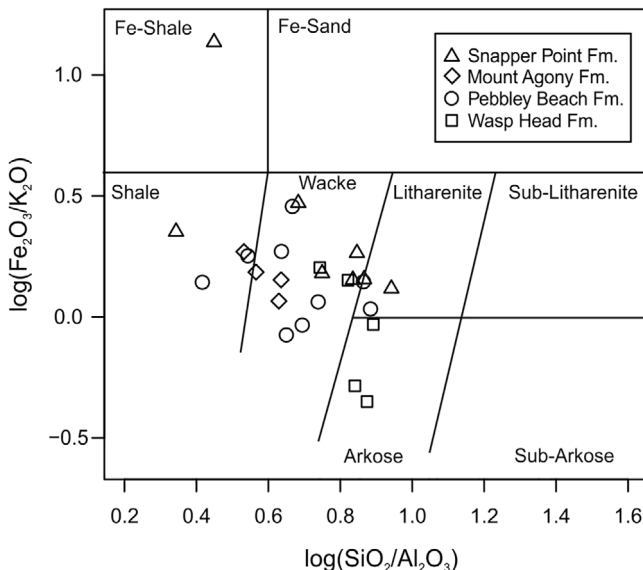


FIGURE 8 Chemical classification scheme for southern Sydney Basin studied samples after Herron (1988)

4.5 | Principal components analysis (PCA)

In order to further examine differences between the studied SSB formations based on major, trace element, and REE contents, a multivariate statistical technique (PCA) was used for detecting possible discrimination patterns based on geochemical variation. A bi-plot illustrating the two most important components detected after PCA was created (Figure 11). In the case of SSB dataset, these components express around 65% of the total geochemical variability of collected samples and can partially separate them in two-dimensional space. Samples characterized by higher amounts of Al_2O_3 , K_2O , MgO , TiO_2 , and some LREE (mainly La, Ce, and Pr) can be distinguished from samples richer in SiO_2 and Na_2O by principal component 1 (PC1). On the other hand, the second most important component (PC2) distinguishes samples richer in Eu, HREE, V, U, Ba, and Sr from samples with higher amounts of Zr and Hf. PC1 separates samples characterized by higher quartz and albite abundances from samples richer in clay minerals, while PC2 distinguishes samples with higher amounts of

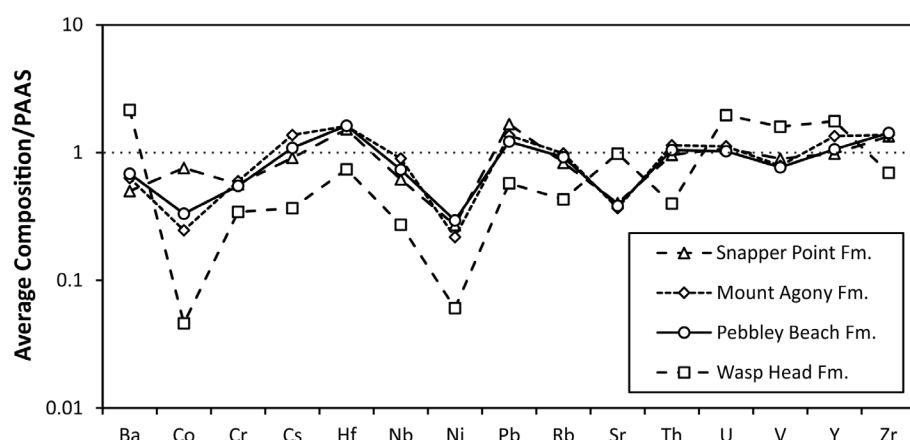


FIGURE 9 Post-Archean Australian Shale (PAAS)-normalized multi-element diagram for trace element concentrations in the studied succession (average values for each formation). PAAS normalizing values from (Condie, 1993; Taylor & McLennan, 1985). The trace element values were normalized as ppm. A horizontal line for a PAAS-normalized value of 1 is included for reference

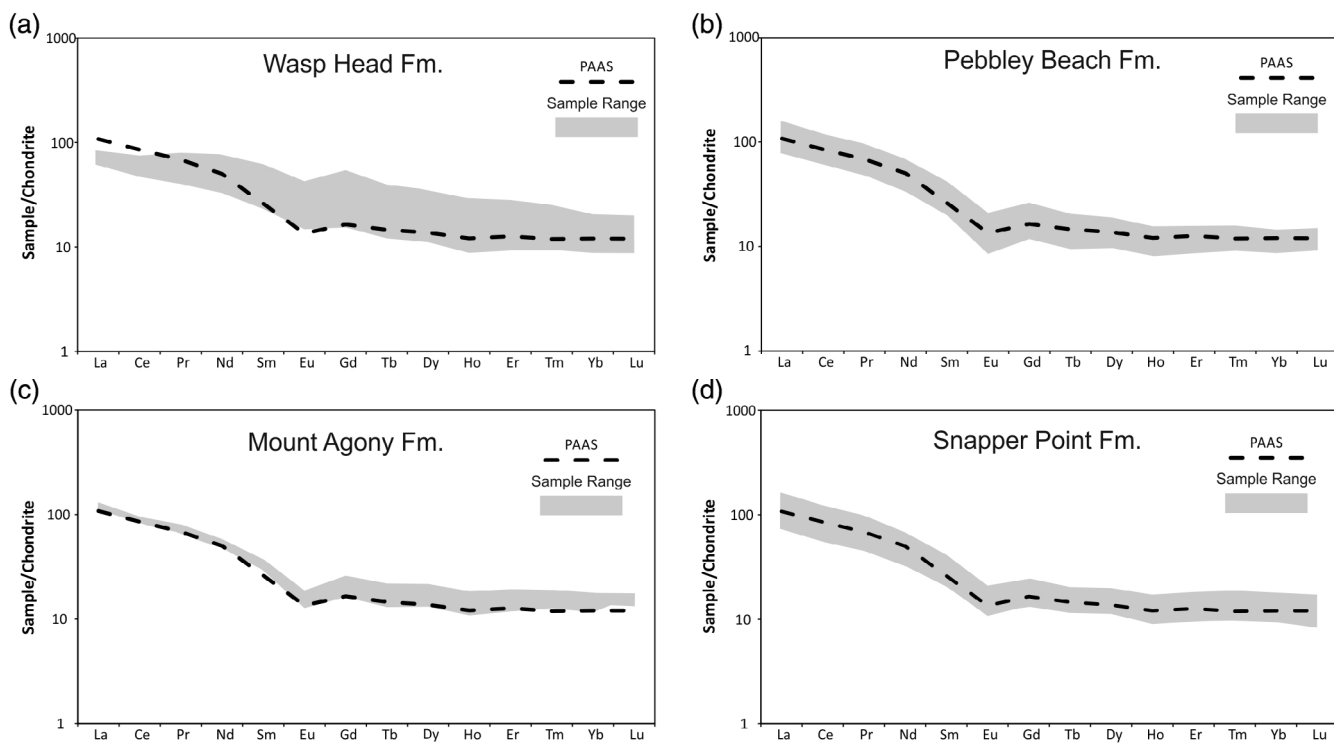


FIGURE 10 Chondrite-normalized rare earth element patterns (sample ranges for each formation). Chondrite normalization values are from Taylor and McLennan (1985). REE pattern of Post-Archean Australian Shale (PAAS) is included for comparison. Note that the Wasp Head Formation (a) exhibits lower LREE contents and displays a lower degree of LREE fractionation along with HREE enrichment, compared with the other three formations (b-d)

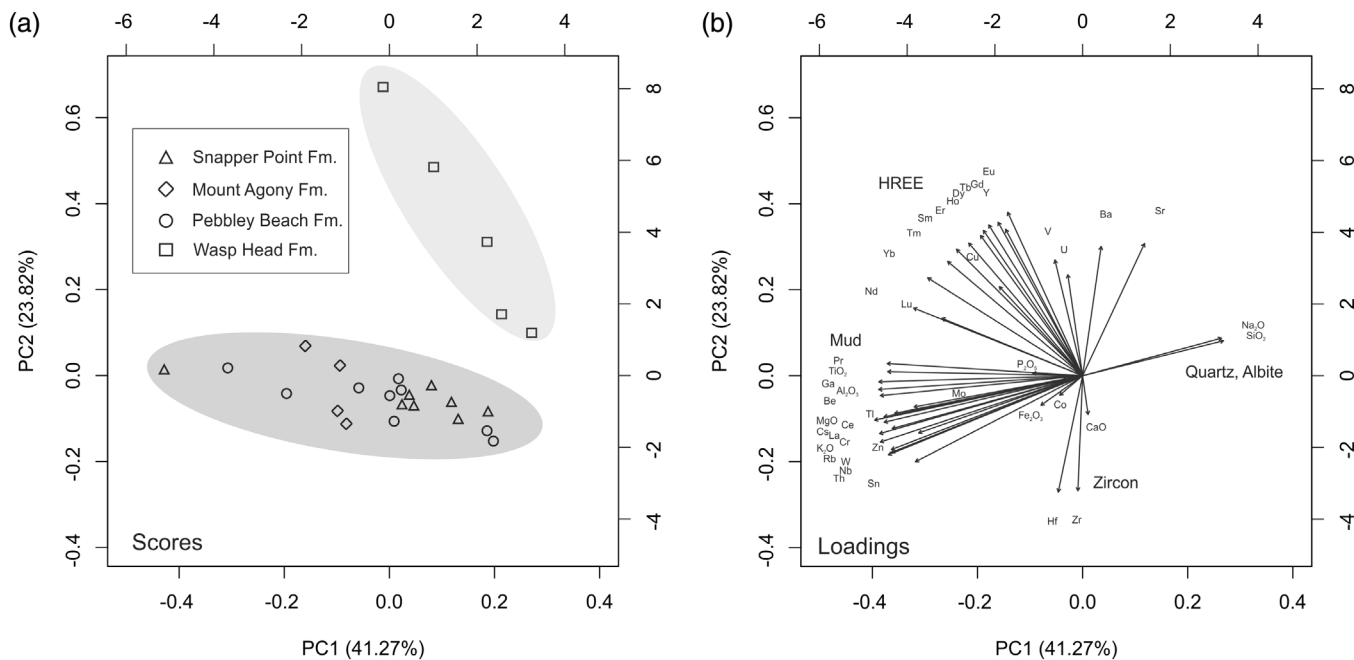


FIGURE 11 PCA scores (a) and loadings (b) plots for major, trace, and rare earth element contents of samples from all studied formations. Wasp Head Formation samples differ from Pebbley Beach, Mount Agony, and Snapper Point formations samples. The latter are seen to be generally poorer in Eu, HREE, V, U, Sr, and Ba and richer in Zr and Hf

zircon and material of more felsic origin (higher contents of Th and Rb), from samples richer in material of more mafic origin (higher contents of HREE, V, Ba, Sr). Figure 11 indicates that the samples from the Pebbley Beach, Mount Agony, and Snapper Point formations are characterized by lower Ba, Sr, V, U, and Eu abundances, compared with the Wasp Head Formation samples (Figure 11a). The PCA reinforces the geochemical distinction between the Wasp Head Formation and all the other formations of the SSB.

5 | DISCUSSION

5.1 | Source rock weathering, sorting, and recycling

The presence of illite in the pore spaces of the studied samples suggests significant weathering that has occurred in the studied sedimentary rocks. Such mixed-layer clays are formed by the breakdown of K-feldspar and plagioclase (particularly the latter) or by the breakdown of unstable lithic fragments. The geochemistry of sedimentary rocks can place constraints on the amount of weathering and sorting, and recycling recorded by the source rocks (Purevjav & Roser, 2013; Tobia & Shangola, 2016). The SSB samples have SiO₂ contents that display negative correlation with Al₂O₃, suggesting hydrodynamic separation of aluminous clays and quartz during deposition (Purevjav & Roser, 2013 and references therein). The strong positive correlation between K₂O and Al₂O₃ suggests that the K occurs in phyllosilicates. Nonetheless, the samples exhibit K₂O/Al₂O₃ ratios below 0.3 and indicate that most K₂O is concentrated in clay minerals (K₂O/Al₂O₃ < 0.3, Cox, Lowe, & Cullers, 1995), rather than in K-feldspar (0.3 < K₂O/Al₂O₃ < 0.9). The positive correlation of Ba and Rb with Al₂O₃ indicates that their distribution is mainly controlled by phyllosilicate minerals (McLennan, Hemming, McDaniel, & Hanson, 1993), especially in the Pebbley Beach and Snapper Point formations (Figure 7b,d). The lack of statistically significant correlation of Th with Al₂O₃ for the Wasp Head and Mount Agony formations indicates that Th is concentrated in an accessory mineral, most likely zircon (Chen et al., 2014), or possibly monazite. The lack of significant correlation between SiO₂ and Zr may indicate that zircon is not abundant, which is clearly the case for the Wasp Head and Mount Agony formations (Figure 7a,c), but for the other formations, it more likely shows the variable concentration of heavy minerals in quartzose sedimentary rocks. The Al₂O₃-V correlation for the Wasp Head Formation is unusual because all other samples show a strong correlation between these elements. However, V is markedly high and Ni distinctly low in the Wasp Head Formation. Usually, these elements follow each other in mafic igneous rocks, with V being concentrated into Ti-Fe oxides (Mongelli, Critelli, Perri, Sonnino, & Perrone, 2006), but the PCA plot shows that no relation exists with Fe, Ti, or Mg. Nevertheless, V concentration could have been increased during sedimentary processes, such as diagenesis (Feng & Kerrich, 1990) or weathering (McLennan, Taylor, & Hemming, 2006). The low Ni, Cr, and Sc concentrations of the Wasp Head Formation samples (around

UCC values) reinforce the idea that V enrichment is related to the above-mentioned processes rather than to the input of a mafic source. The overall negative correlation between Al₂O₃-Ni for the Wasp Head Formation suggests that the distribution of Ni bears little or no relationship to the clays and contents are controlled by the concentration in heavy minerals or relict mafic minerals.

The degree of source rock weathering is evaluated by using: (a) the correlation of Al₂O₃ with TiO₂. Less well correlated trends are indicative of lower degree of weathering (Young & Nesbitt, 1999). (b) The chemical index of alteration (CIA = molar [Al₂O₃ / (Al₂O₃ + CaO* + Na₂O + K₂O)]) × 100; Nesbitt & Young, 1982), which evaluates the extent of conversion of plagioclase and K-feldspars (CIA = 50) to aluminous clays (CIA ≤ 100). Severely weathered rocks record high CIA values (Nesbitt & Young, 1982). The maturity of the source material of sedimentary rocks is evaluated by using the index of compositional variability (ICV = (Fe₂O₃ + K₂O + Na₂O + CaO + MgO + MnO + TiO₂) / Al₂O₃), with mature rocks being characterized by higher Al₂O₃ and lower ICV values (Cox et al., 1995). Low ICV values (<1) are also associated with higher degree of source rock weathering (Cox et al., 1995). A mature source and a moderate to strong degree of source weathering are suggested for the studied Lower Permian deposits in the SSB, based on the ICV (mean 0.73), CIA (mean 73.3) values, and the strong positive correlation of Al₂O₃ with TiO₂ (Figure 12a).

Similar conclusions can be reached by the Al₂O₃ – CaO* + Na₂O – K₂O (A-CN-K) ternary diagram of Nesbitt and Young (1984), which is utilized to estimate weathering intensity (Figure 12b). The A-CN-K ternary diagram takes into consideration the relative contributions of Al₂O₃ (aluminous clays), CaO + Na₂O (plagioclase), and K₂O (K-feldspar) in sedimentary rocks. In this plot, CaO* is referred to that occurring in silicate minerals (excluding calcite, dolomite, and apatite). If CaO < Na₂O, the molecular CaO is considered as approximate CaO* (McLennan et al., 1993). This condition applies to all SSB samples. In this plot, samples of different source rock compositions that plot close to the Pl-Ks tie line indicate low levels of weathering (Nesbitt & Young, 1984). The movement towards the A axis is indicative of more intense weathering and is the result of the breakdown of plagioclase to kaolinite. In cases of post-depositional K-metasomatism, the weathering trend line deviates from the predicted line and moves to the K₂O apex (Nesbitt & Young, 1984). The SSB samples plot towards the Al₂O₃ apex and along the predicted weathering trend, forming a sub-parallel line to the A-CN side. These features indicate moderate to strong degree of source weathering (Figure 12b).

Further processes involved in determining the sediment sorting and recycling of the SSB deposits have been ascertained from the Al₂O₃-Zr-TiO₂ diagram. It is considered that mature sedimentary rocks exhibit a wide range of TiO₂/Zr variation, in contrast to immature sedimentary rocks (Garcia, Coehlo, & Perrin, 1991). The samples from the Wasp Head Formation plot close to the PAAS suggesting lower degree of recycling (Figure 13a). In contrast, samples from the other formations follow the recycling trend, suggesting higher degree of source sorting and sediment recycling. This might be expected, as the Wasp Head Formation is the basal and oldest sedimentary unit of

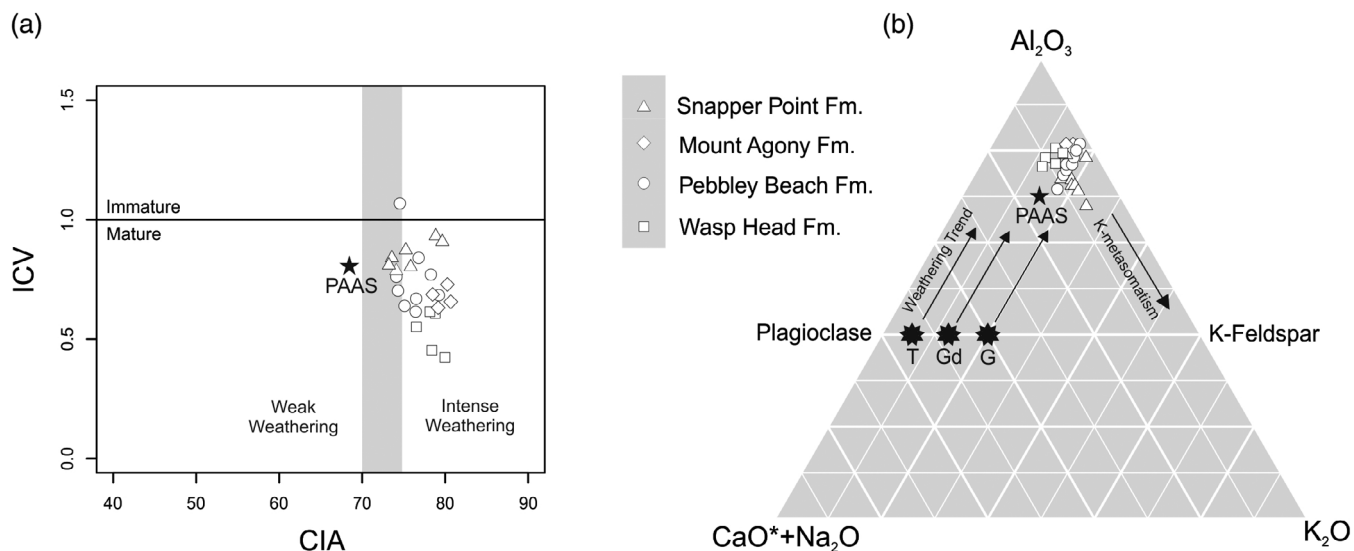


FIGURE 12 (a) CIA versus ICV diagram for the southern Sydney Basin sedimentary rocks (after Cox et al., 1995; Nesbitt & Young, 1984). Grey field represents the CIA range of Phanerozoic shale (after Long, Sun, Yuan, Xiao, & Cai, 2008). PAAS composition taken from Taylor and McLennan (1985). (b) A-CN-K diagram for the southern Sydney Basin sedimentary rocks. Average tonalite (T), granodiorite (Gd), and granite (G) compositions shown are taken from Condie (1993). Predicted weathering trends (arrows) of T, Gd, and G are also shown

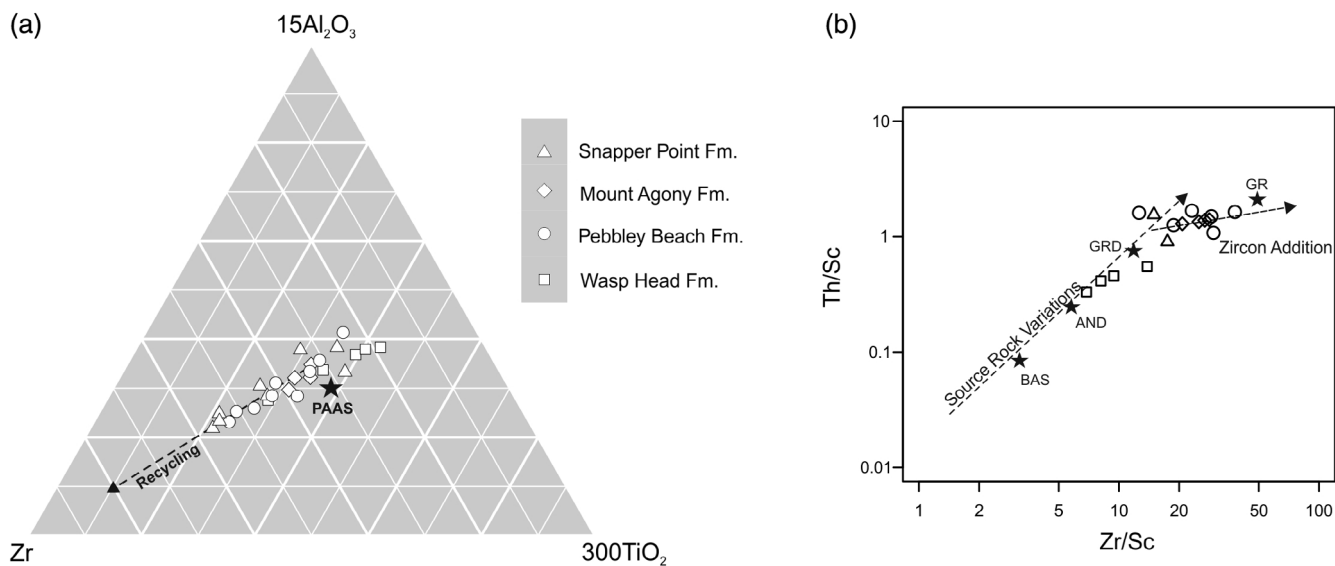


FIGURE 13 (a) $15\text{Al}_2\text{O}_3$ -Zr- 300TiO_2 ternary diagram (Garcia et al., 1991). (b) Th/Sc versus Zr/Sc diagram that evaluates the source rock composition of the studied sediments (McLennan et al., 1993). BAS, AND, GRD, and GR refer to average gabbro, andesite, granodiorite, and granite, respectively (Le Maitre, 1976)

the SSB and has undergone less transportation distance than the other overlying formations and accumulated in a depositional area closer to the source. This interpretation is further supported by the predominance of very angular to angular clasts in conglomeratic deposits of the Wasp Head Formation (Figure 4a).

Summarizing, the geochemistry of the studied deposits indicates a generally moderate to strong degree of source weathering for the SSB samples. Furthermore, the oldest sedimentary rocks (Wasp Head Formation) are less-weathered and less-affected by sorting and

sediment recycling, compared to the younger deposits (Pebbley Beach, Mount Agony, and Snapper Point formations).

5.2 | Provenance

Throughout the studied formations, monocrystalline and polycrystalline quartz, plagioclase, K-feldspar, composite quartz-feldspar grains, uncommon hornblende, and tourmaline occur. This combination

suggests derivation from magmatic and probably granitic source (Götze & Möckel, 2012). Further, tourmaline can also be derived from low- and high-grade metamorphic rocks (Mange & Maurer, 1992). Derivation from rocks that have been deformed and recrystallised under low grade, metamorphic conditions is also suggested by the undulose extinction of quartz grains and presence of polycrystalline quartz. Further, other sources are suggested by the types of lithic fragments. These consist of felsic volcanic as well as low-grade metamorphic (meta-siltstone, slate, and quartzite) and sedimentary rocks (chert, siliceous, and radiolarian-bearing lutite) indicating that at least three sources have provided the detritus for the sedimentary rocks in the formations. This interpretation agrees with the results presented by Gostin (1968), who additionally noticed that the Wasp Head Formation was sourced by different rock types, compared with the other formations. The Wasp Head Formation originates from sedimentary and low-grade metamorphic source rocks, whereas the other formations were sourced from a granitic-volcanic terrain (Gostin, 1968). This compositional difference between Wasp Head Formation and the other formations is further reflected in the geochemistry of the samples.

The moderate to high $\text{Al}_2\text{O}_3/\text{TiO}_2$ ratios (ca. 20), and the TiO_2 versus Al_2O_3 plot suggest that the detritus in most formations has been derived from felsic to intermediate rocks, those with lower $\text{Al}_2\text{O}_3/\text{TiO}_2$ ratios from more mafic rocks. The samples from the Pebbley Beach, Mount Agony, and Snapper Point formations are more enriched in LREE (higher $\text{La}_{\text{N}}/\text{Yb}_{\text{N}}$ ratios) and have flatter HREE segments than those from the Wasp Head Formation, indicating a more felsic source rock signature (Figure 10). Further evidence for the contribution of a mafic component in the Wasp Head Formation comes from the $\text{Gd}_{\text{N}}/\text{Yb}_{\text{N}}$ ratios and the Eu anomalies. The samples from the Wasp Head Formation exhibit smaller negative Eu anomalies and greater $\text{Gd}_{\text{N}}/\text{Yb}_{\text{N}}$ ratios than the samples from the other formations. Further, the A-CN-K plot (Figure 12b) suggests derivation from source rocks with an average composition close to granite, except for the Wasp Head Formation that is less felsic (close to granodiorite). In the plot of Th/Sc versus Zr/Sc , the samples from the Wasp Head Formation display lower Th/Sc values than the samples from the other formations, suggesting derivation from intermediate igneous sources (Figure 13b). The plot based on samples PCA scores also indicates that the Wasp Head Formation is geochemically separated from the other three formations by higher contents of HREE, U, V, Sr, and Ba and lower contents of elements such as Zr, La, Th, and Rb (Figure 11). The lower Th, Zr, and Rb contents are reflection of the source rocks, probably andesites in the Wasp Head Formation. Samples from the Pebbley Beach, Mount Agony, and Snapper Point formations cannot be easily distinguished based on PCA analysis, but it appears that the majority of Snapper Point Formation samples are less mud-rich and more quartz-rich than their Pebbley Beach and Mount Agony formations counterparts.

Summarising, the geochemistry of the SSB deposits and the statistical analysis agree with the petrographic analysis of Gostin (1968), suggesting that the basal and oldest formation (Wasp Head Formation) is compositionally different, compared with all the other

formations. The current study indicates that the samples from the Wasp Head Formation preserve a more mafic/andesitic signature, and those from the overlying Pebbley Beach, Mount Agony, and Snapper Point formations preserve a granodioritic/dacitic signature.

5.3 | Tectonic setting

Several geochemically-based diagrams for the tectonic discrimination of siliciclastic sedimentary rocks exist (e.g., Bhatia, 1983; Gorton & Shandl, 2000; McLennan, 1989; Roser & Korsch, 1986; Verma & Armstrong-Altrin, 2013) that have been recently applied (e.g., Tao, Sun, Wang, Yang, & Jiang, 2014; Tawfik et al., 2017). The discrimination diagrams of Bhatia (1983) and Roser and Korsch (1986) have been proven to be inconsistent with tectonic settings based on regional geology (Dostal & Keppie, 2009; Valloni & Maynard, 1981), and have been questioned by several authors (Armstrong-Altrin & Verma, 2005; Ryan & Williams, 2007; Verma & Armstrong-Altrin, 2013; Verma, Pandarinath, Verma, & Agrawal, 2013).

Verma and Armstrong-Altrin (2013) introduced a new discriminant-function-based major-element diagram for high-silica ($\text{SiO}_2 = 63\text{--}95\%$) and low-silica ($\text{SiO}_2 = 35\text{--}63\%$) sedimentary rocks to establish the tectonic setting of sedimentary basins. This diagram distinguishes island or continental arc, continental rift and collisional settings. It is based on results from Neogene to Quaternary deposits, but also has been employed on older sedimentary rocks (Tawfik et al., 2017; Zaid & Gahtani, 2015). Another plot that separates active from passive margins uses all major element contents (Verma & Armstrong-Altrin, 2016). The active margin field encompasses collisional and arc-related tectonic settings, and the passive margin field corresponds to rift settings. On both the high- and low-silica multidimensional diagrams, the samples from the entire sequence in the study area plot in the rift field and indicate regional extension (Figure 14a,b). Similar conclusions come from the major element-based diagram, where all samples plot on the passive margin field (Figure 14c). This rift-type origin of the SSB confirms the extensional setting proposed by other authors (references herein) for the Early Permian deposits.

Despite the usefulness of petrographic and geochemical studies in the analysis of sedimentary basins, the tectonic setting must be verified by the actual regional sedimentary record and thus the interpretation requires a multi-disciplinary approach and consideration of different types of evidence (Maravelis, Boutelier, Catuneanu, Seymour, & Zelilidis, 2016; Ryan & Williams, 2007). The discrimination diagrams of Verma and Armstrong-Altrin (2013) and Verma and Armstrong-Altrin (2016) indicate deposition in an intercontinental rift basin, and this conclusion fits well with the basin-fill conditions in the SSB. The sequence stratigraphic framework indicates either a continuous deepening upwards trend (Maravelis et al., 2018) or a more complicated pattern involving several deepening- and shallowing-upwards trends (Fielding et al., 2006; Rygel et al., 2008). Despite these different interpretations that could largely stem from the different scale of observation (e.g., Catuneanu, 2018), both scenarios suggest a

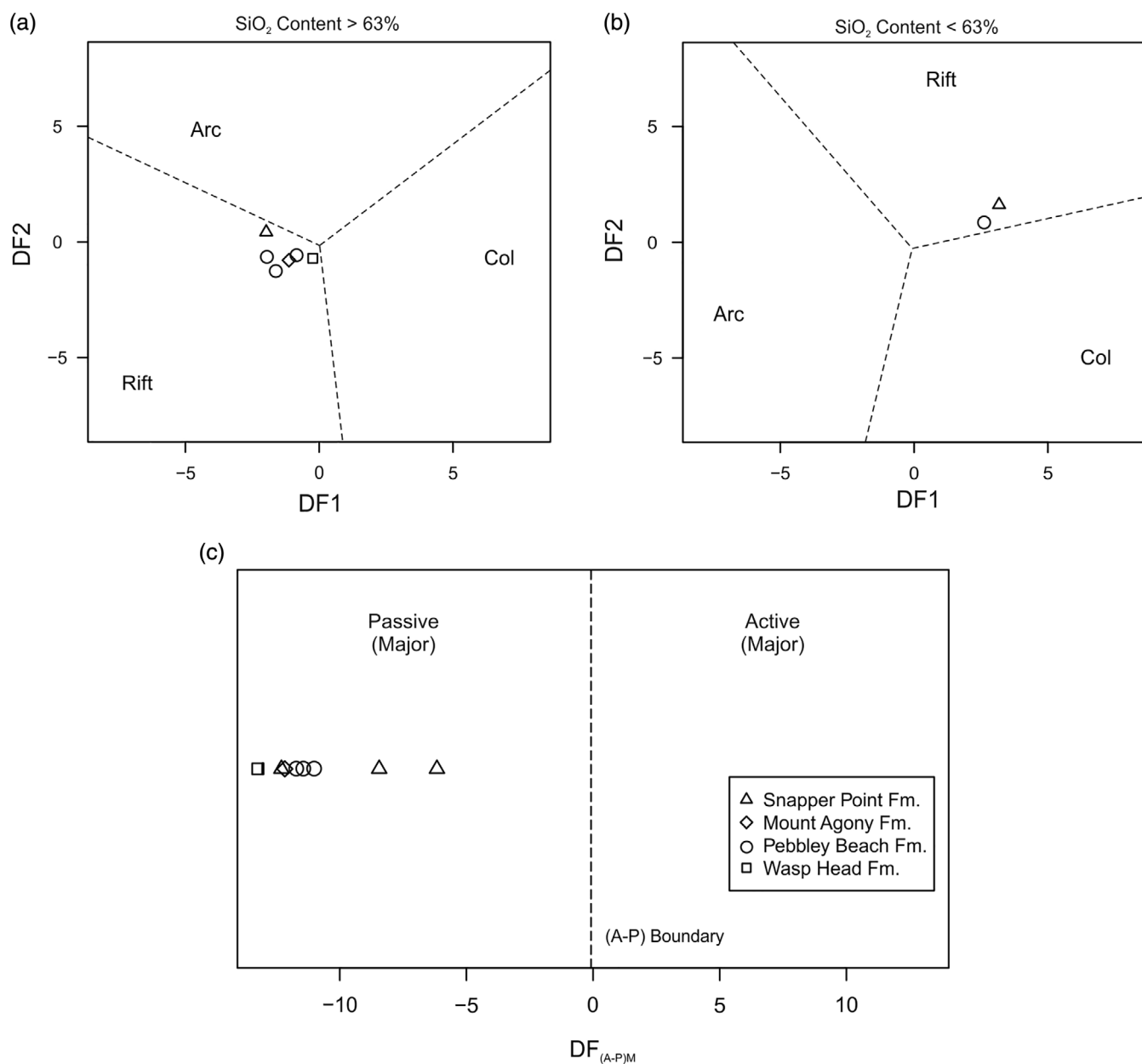


FIGURE 14 Binary diagrams that evaluate the geotectonic setting of the studied succession. Discriminant function multi-dimensional plots for (a) high-silica and (b) low-silica clastic sediments (for a detailed description of the discriminant-function equations, see Verma & Armstrong-Altrin, 2013). (c) Major element-based discriminant function diagram that separates active (A) and passive (P) margins (from Verma & Armstrong-Altrin, 2016). Samples with MnO contents below the detection limit were not plotted

temporal deepening-upwards trend (from Wasp Head to Snapper Point Formation). This trend is compatible with a sedimentary succession deposited within a rift-type basin.

5.4 | Early Permian geotectonic implications

The geochemical data presented in this study suggest that the SSB served as a rift-type basin during the Early Permian. This extensional setting is compatible with the regional tectonic activity and the Denison Event (Korsch, Boreham, Totterdell, Shaw, & Nicoll, 1998), which

is responsible for the: (a) Early Permian East Australian Rift System that occurs along the eastern margin of Australia, (b) uplift of the Lachlan orogeny, and (c) development of the SSB (Korsch et al., 2009; Tye et al., 1996). Zircon analyses indicate that the onset of rifting and the extensional event in the Sydney Basin took place at 299 Ma (Shaanan et al., 2015; Vevers, 2013). Supporting evidence for a rift-type setting comes from the published sequence stratigraphic framework that suggests control of tectonically-induced subsidence on sedimentation (e.g., Fielding et al., 2006; Maravelis et al., 2018; Rygel et al., 2008; Tye et al., 1996). Additional parameters include the high sedimentation rates and the high topographic gradients

(Maravelis et al., 2018). Published palaeocurrent data derived from cross-stratification and clast imbrications in the Wasp Head Formation suggest a generally consistent pattern of transport and a principal eastwards flow direction (Rygel et al., 2008), with a less common westwards direction (Gostin & Herbert, 1973; Rygel et al., 2008). Palaeocurrent analysis from the Pebbley Beach Formation suggests a bi-modal to bi-polar distribution, with a significant south-westward and east trend and a lateral accretion trend to the east (Fielding et al., 2006). This pattern agrees with the temporal changes observed in rift-type basins (Dalrymple & Choi, 2007), indicating that the uplifted shoulder of the rift is positioned to the west. This result makes the Lachlan orogen as the most suitable source area and agrees with the provenance results presented in this study.

The petrographic and geochemical analyses reveal that the detritus in the SSB samples was derived from diverse rock types, including felsic volcanic, plutonic, sedimentary, and low-grade metamorphic rocks. Several potential regional source-area candidates responsible for the majority of the detritus occur in the Lachlan orogen. The source rocks for the Wasp Head Formation are most likely represented by the Ordovician Adaminaby Group that is a large submarine fan system, widespread in the Lachlan orogen, and could be sedimentary source of the studied formations. This is supported by the presence of sandstone and mudstone clasts in the conglomeratic deposits of the Wasp Head Formation (Gostin & Herbert, 1973), and the abundance of chert clasts within the sandstone samples. Another type of detritus observed in the Wasp Head Formation has been obtained from a low-grade metamorphic terrane that included meta-siltstone, slate, and quartzite. The likely source of these rock types is the Watonga Group in the Narooma accretionary complex because it contains these types of rocks (Gostin, 1968; Prendergast, Offler, Phillips, & Zwingmann, 2011).

The potential source rock candidates for the other formations include the Ordovician, high-K calc-alkaline, and shoshonitic volcanic, and less common plutonic rocks in the Macquarie Arc (Figure 1; Crawford, Meffre, Squire, Barron, & Falloon, 2007 and references therein), and the Silurian–Devonian felsic and mafic volcanic rocks of the Comerong Volcanics that formed in intra-continental rift settings (Atton, 2013; Dadd, 2011), because the SSB samples show similarities to these rocks (e.g., LREE- and Th-enriched, and Nb-depleted patterns). However, the Ordovician volcanic rocks are dominantly mafic, have lower Th contents, and lack well-developed sub-continental lithosphere in contrast to the SSB deposits and thus are unlikely to provide most of the detritus for the SSB. It is more likely that the Silurian–Devonian volcanic rocks and volcanogenic sequences have been the dominant contributors because they are moderately widespread in the eastern Lachlan orogeny and are dominantly felsic and exhibit within plate enrichment (Atton, 2013; Dadd, 2011). However, granite boulders have been observed in the Early Permian successions indicating that Silurian and Devonian granites in the Lachlan orogen have contributed detritus (Gostin, 1968). The presence of orthoclase grains in the sandstones (Gostin, 1968) supports this interpretation.

6 | CONCLUSIONS

Geochemical and petrographic results of the present study combined with published sedimentological and stratigraphic analyses of the Lower Permian sedimentary rocks in the SSB have provided insights into the provenance and tectonic setting of the SSB deposits.

Petrographic analysis agrees with previous studies, which demonstrate that sandstone samples from the Wasp Head Formation are lithic arenites and the sandstone from the other formations ranges between feldspatho-lithic, litho-feldspathic, and sub-labile arenites. The sandstone from the Wasp Head Formation contains detritus derived mainly from low-grade metamorphic and sedimentary rocks, whereas the sandstone from the other formations originated from felsic volcanic and plutonic rocks. Major element characteristics revealed that the samples: (a) can be classified as shales, wackes, litharenites, and arkoses, (c) are geochemically mature, and (c) originated from a source with moderate to strong degree of weathering, as indicated by the ICV and CIA values (mean 0.73 and 73.3, respectively). The trace and REE contents and different trace element ratios of the samples revealed that the detritus originated principally from felsic source rocks (for Pebbley Beach, Mount Agony, and Snapper Point formations), and from intermediate rocks for the oldest (basal) rocks (Wasp Head Formation). Discrimination diagrams indicated that the formations were deposited in a rift-type setting. This interpretation is consistent with the geology of the SSB and the published sequence stratigraphic framework that indicates a general deepening-upward trend and the development of a depositional sequence with an asymmetric, principally transgressive architecture. Previous analyses suggest that the palaeocurrent directions are to the east, indicating that the source area is positioned to the west.

The integration of provenance data reported here, in conjunction with previous palaeocurrent and sequence stratigraphic analysis, suggests that the Lachlan orogen is the principal sediment contributor in the SSB. Most of the detritus was most likely derived from the Devonian felsic and mafic volcanic rocks that formed in intra-continental rift settings and Devonian and Silurian granites. Other potential source areas were the rocks in the Cambrian–Ordovician Wagonga Group of the Narooma accretionary complex and the Ordovician Adaminaby Group.

ACKNOWLEDGEMENTS

This study is part of the research project: Palaeogeographic and geotectonic evolution of the Myall Trough and Sydney Basin: Constraints in the Palaeozoic geological history of eastern Australia, co-funded by the NSW Institute for Frontiers Geoscience (IFG). The authors wish to thank the journal editor (John Armstrong-Altrin) and the three anonymous reviewers for constructive criticism that greatly improved the manuscript. Yanyan Sun (UoN) is thanked for preparing the thin sections. Dr. Bill Landenberger is acknowledged for insightful discussions regarding the geodynamics of the Sydney Basin. The authors are indebted to the Office of Environment and Heritage, NSW National Parks and Wildlife Service for providing us permission to sample rocks in the National Park.

DATA AVAILABILITY STATEMENT

Petrographic data used in this article were compiled from Gostin (1968) after the author's permission. Our new petrographic and geochemical data are available as Supporting Information tables.

ORCID

George Pantopoulos  <https://orcid.org/0000-0002-3655-246X>

REFERENCES

- Alder, J. D., Hawley, S., Maung, T., Scott, J., Shaw, R. D., Sinelnikov, A., & Kouzmina, G. (1998). Prospectivity of the offshore Sydney Basin: A new perspective. *APPEA Journal*, 38, 68–92.
- Armstrong-Altrin, J. S. (2009). Provenance of sands from Cazones, Acapulco, and Bahía Kino beaches, México. *Revista Mexicana de Ciencias Geológicas*, 26, 764–782.
- Armstrong-Altrin, J. S., & Verma, S. P. (2005). Critical evaluation of six tectonic setting discrimination diagrams using geochemical data of Neogene sediments from known tectonic settings. *Sedimentary Geology*, 177, 115–129.
- Atton, H. (2013). *Tectono-metallogenetic evolution of Silurian to Devonian felsic volcanics of the Lachlan Orogen, Orange Region*. (Bachelor of Science [Honours]). School of Earth and Environmental Science, University of Wollongong, Australia, 1–158. <https://ro.uow.edu.au/thsci/58>.
- Babaahmadi, A., Sliwa, R., Esterle, J., & Rosenbaum, G. (2017). The development of a Triassic fold-thrust belt in a synclinal depositional system, Bowen Basin (eastern Australia). *Tectonics*, 36(1), 51–77.
- Bauluz, B., Mayayo, M. J., Fernandez-Nieto, C., & Gonzalez Lopez, J. M. (2000). Geochemistry of Precambrian and Paleozoic siliciclastic rocks from the Iberian Range (NE Spain): Implications for source-area weathering, sorting, provenance, and tectonic setting. *Chemical Geology*, 168, 135–150.
- Bhatia, M. R. (1983). Plate tectonics and geochemical composition of sandstones. *Journal of Geology*, 91, 611–627.
- Briggs, D. J. C. (1998). *Permian Productidina and Strophalosiidina from the Sydney-Bowen Basin and New England orogen: systematics and biostratigraphic significance* (Vol. 19). Canberra: Association of Australasian Palaeontologists 258 pp.
- Campbell, M. J., Shaanan, U., & Verdel, C. (2017). Fold-interference patterns in the Bowen Basin, northeastern Australia. *Australian Journal of Earth Sciences*, 64(5), 577–585.
- Catuneanu, O. (2018). Model-independent sequence stratigraphy. *Earth-Science Reviews*, 188, 312–388.
- Catuneanu, O., Hancox, P. J., Cairncross, B., & Rubidge, B. S. (2002). Foredeep submarine fans and forebulge deltas: Orogenic off-loading in the underfilled Karoo Basin. *Journal of African Earth Sciences*, 35, 489–502.
- Cawood, P. A. (2005). Terra Australis orogen: Rodinia breakup and development of the Pacific and Iapetus margins of Gondwana during the Neoproterozoic and Paleozoic. *Earth-Science Reviews*, 69, 249–279.
- Chen, M., Sun, M., Cai, K., Buslov, M. M., Zhao, G., & Rubanova, E. S. (2014). Geochemical study of the Cambrian-Ordovician meta-sedimentary rocks from the Altai-Mongolian terrane, northwestern Central Asian Orogenic Belt: Implications on the provenance and tectonic setting. *Journal of Asian Earth Sciences*, 96, 69–83.
- Collins, W. J. (1991). A reassessment of the 'Hunter-Bowen Orogeny': Tectonic implications for the southern New England fold belt. *Australian Journal of Earth Sciences*, 38, 409–423.
- Condie, C. K. (1993). Chemical composition and evolution of the upper continental crust: Contrasting results from surface samples and shales. *Chemical Geology*, 104, 1–37.
- Condie, C. K., Noll, P. D., Jr., & Conway, C. M. (1992). Geochemical and detrital mode evidence for two sources of Early Proterozoic sedimentary rocks from the Tonto Basin Supergroup, central Arizona. *Sedimentary Geology*, 77, 51–76.
- Cox, R., Lowe, D. R., & Cutters, R. (1995). The influence of sediment recycling and basement composition on evolution of mudrock chemistry in the southwestern United States. *Geochimica et Cosmochimica Acta*, 59, 2919–2940.
- Crawford, A. J., Meffre, S., Squire, R. J., Barron, L. M., & Falloon, T. J. (2007). Middle and Late Ordovician magmatic evolution of the Macquarie Arc, Lachlan orogen, New South Wales. *Australian Journal of Earth Sciences*, 54, 181–214.
- Crook, K. A. W. (1960). Classification of arenites. *American Journal of Science*, 258, 419–428.
- Dadd, K. A. (2011). Extension-related volcanism in the Middle to Late Devonian of the Lachlan orogen: Geochemistry of mafic rocks in the Comerong Volcanics. *Australian Journal of Earth Sciences*, 58, 209–222.
- Dalrymple, R. W., & Choi, K. (2007). Morphologic and facies trends through the fluvial-marine transition in tide-dominated depositional systems: A schematic framework for environmental and sequence-stratigraphic interpretation. *Earth-Science Reviews*, 81, 135–174.
- Dimalanta, C. B., Faustino-Eslava, D. V., Padrones, J. T., Queaño, K. L., Concepcion, R. A. B., Suzuki, S., & Yumul, G. P., Jr. (2018). Cathaysian slivers in the Philippine island arc: Geochronologic and geochemical evidence from sedimentary formations of the west Central Philippines. *Australian Journal of Earth Sciences*, 65, 93–108.
- Dostal, J., & Keppie, J. D. (2009). Geochemistry of low-grade clastic rocks in the Acatlán Complex of southern Mexico: Evidence for local provenance in felsic intermediate igneous rocks. *Sedimentary Geology*, 222, 241–253.
- Egozcue, J. J., Pawlowsky-Glahn, V., Mateu-Figueras, G., & Barceló-Vidal, C. (2003). Isometric log ratio transformations for compositional data analysis. *Mathematical Geology*, 35, 279–300.
- Eyles, C. H., Eyles, N., & Gostin, V. A. (1998). Facies and allostratigraphy of high-latitude, glacially influenced marine strata of the Early Permian southern Sydney Basin, Australia. *Sedimentology*, 45, 121–161.
- Feng, R., & Kerrich, R. (1990). Geochemistry of fine-grained clastic sediments in the Archean Abitibi greenstone belt, Canada: Implications for provenance and tectonic setting. *Geochimica et Cosmochimica Acta*, 54, 1061–1081.
- Fielding, C. R., Bann, K. L., MacEachern, J. A., Tye, S. C., & Jones, B. G. (2006). Cyclicity in the nearshore marine to coastal, Lower Permian, Pebbley Beach Formation, southern Sydney Basin, Australia: A record of relative sea-level fluctuations at the close of the late Palaeozoic Gondwanan ice age. *Sedimentology*, 53, 435–463.
- Garcia, D., Coehlo, J., & Perrin, M. (1991). Fractionation between TiO₂ and Zr as a measure of sorting within shale and sandstone series (northern Portugal). *European Journal of Mineralogy*, 3, 401–414.
- Glen, R. A. (2005). The Tasmanides of Eastern Australia: 600 million years of interaction between the proto-Pacific plate and the Australian sector of Gondwana. In A. P. M. Vaughan, P. T. Leat, & R. J. Pankhurst (Eds.), *Terrane processes at the margins of Gondwana* (Vol. 246, pp. 23–96). London, England: Geological Society, Special Publication.
- Glen, R. A. (2013). Refining accretionary orogen models for the Tasmanides of eastern Australia. *Australian Journal of Earth Sciences*, 60, 315–370.
- Gorton, M. P., & Shandl, E. S. (2000). From continents to island arcs: A geochemical index of tectonic setting for arc-related and within-plate felsic to intermediate volcanic rocks. *Canadian Mineralogist*, 38(5), 1065–1073.
- Gostin, V. A. (1968). *Stratigraphy and sedimentology of the Lower Permian sequence in the Durras-Ulladulla area, Sydney Basin, New South Wales*. (PhD thesis). Australian National University, Canberra, Australia, 1–160.
- Gostin, V. A., & Herbert, C. (1973). Stratigraphy of the Upper Carboniferous and Lower Permian sequence, southern Sydney Basin. *Journal of the Geological Society of Australia*, 20, 49–70.

- Götze, J., & Möckel, R. (2012). *Quartz: deposits, mineralogy and analytics*. Berlin: Springer pp. 1–360.
- Herbert, C., & Helby, R. (1980). *A guide to the Sydney Basin*. Sydney: Geological Survey of New South Wales 1–603.
- Herron, M. M. (1988). Geochemical classification of terrigenous sands and shales from core or log data. *Journal of Sedimentary Petrology*, 58, 820–829.
- Holcombe, R. J., Stephens, C. J., Fielding, C. R., Gust, D., Little, T. A., Sliwa, R., ... Ewart, A. (1997). Tectonic evolution of the northern New England Fold Belt: The Permian-Triassic Hunter-Bowen event. In P. M. Ashley & P. G. Flood (Eds.), *Tectonics and metallogenesis of the New England Orogen* (Vol. 19, pp. 52–65). London, Sydney: Geological Society of Australia, Special Publication.
- Hoy, D., & Rosenbaum, G. (2017). Episodic behavior of Gondwanide deformation in eastern Australia: Insights from the Gympie Terrane. *Tectonics*, 36(8), 1497–1520.
- Hutton, A. C. (2009). Geological setting of Australasian coal deposits. In R. Kininmonth & E. Baafi (Eds.), *Australasian coal mining practice* (pp. 40–84). Melbourne, Victoria: Australasian Institute of Mining and Metallurgy.
- Jenkins, R. B., Landenberger, B., & Collins, W. J. (2002). Late Palaeozoic retreating and advancing subduction boundary in the New England Fold Belt, New South Wales. *Australian Journal of Earth Sciences*, 49, 467–489.
- Korsch, R. J., Boreham, C. J., Totterdell, J. M., Shaw, R. D., & Nicoll, M. G. (1998). Development and petroleum resource evaluation of the Bowen, Gunnedah and Surat Basins, eastern Australia. *APPEA Journal*, 38, 199–236.
- Korsch, R. J., Totterdell, J. M., Cathro, D. L., & Nicoll, M. G. (2009). Early Permian East Australian rift system. *Australian Journal of Earth Sciences*, 56, 381–400.
- Le Maitre, R. W. (1976). The chemical variability of some common igneous rocks. *Journal of Petrology*, 17, 589–598.
- Le Roux, J. P., & Jones, B. G. (1994). Lithostratigraphy and depositional environment of the Permian Nowra Sandstone in the southwestern Sydney Basin, Australia. *Australian Journal of Earth Sciences*, 41, 191–203.
- Long, X., Sun, M., Yuan, C., Xiao, W., & Cai, K. (2008). Early Paleozoic sedimentary record of the Chinese Altai: Implications for its tectonic evolution. *Sedimentary Geology*, 208, 88–100.
- Mange, M. A., & Maurer, H. F. W. (1992). *Heavy minerals in color*. London: Chapman and Hall 147 pp.
- Maravelis, A. G., Boutelier, D., Catuneanu, O., Seymour, K. S., & Zelilidis, A. (2016). A review of tectonics and sedimentation in a forearc setting: Hellenic Thrace Basin, north Aegean Sea and northern Greece. *Tectonophysics*, 674, 1–19.
- Maravelis, A. G., Catuneanu, O., Nordsvan, A., Landenberger, B., & Zelilidis, A. (2018). Interplay of tectonism and eustasy during the Early Permian icehouse: Southern Sydney Basin, southeast Australia. *Geological Journal*, 53, 1372–1403.
- Maravelis, A. G., Chamaki, E., Pasadakis, N., Zelilidis, A., & Collins, W. J. (2017). Hydrocarbon generation potential of a Lower Permian sedimentary succession (Mount Agony Formation): Southern Sydney Basin, New South Wales, Southeast Australia. *International Journal of Coal Geology*, 183, 52–64.
- Maravelis, A. G., Pantopoulos, G., Tseras, P., & Zelilidis, A. (2015). Accretionary prism-forearc interactions as reflected in the sedimentary fill of southern Thrace Basin (Lemnos Island, NE Greece). *International Journal of Earth Sciences*, 104(4), 1039–1060.
- McLennan, S. M. (1989). Rare earth elements in sedimentary rocks: Influence of provenance and sedimentary process. In B. R. Lipin & G. A. McKay (Eds.), *Geochemistry and mineralogy of rare earth elements* (Vol. 21, pp. 169–200). Washington, DC: Mineralogical Society of America, Reviews in Mineralogy.
- McLennan, S. M., Hemming, S., McDaniel, D. K., & Hanson, G. N. (1993). Geochemical approaches to sedimentation, provenance and tectonics. In M. J. Johnson & A. Basu (Eds.), *Processes controlling the composition of clastic sediments* (Vol. 284, pp. 21–40). Boulder, Colorado: Geological Society of America Special Paper.
- McLennan, S. M., Taylor, S. R., & Hemming, S. (2006). Composition, differentiation, and evolution of continental crust: Constraints from sedimentary rocks and heat flow. In M. Brown & T. Rushmer (Eds.), *Evolution and differentiation of the continental crust* (pp. 92–134). Cambridge: Cambridge University Press.
- McLennan, S. M., Taylor, S. R., McCulloch, M. T., & Maynard, J. B. (1990). Geochemical and Nd-Sr isotopic composition of deep-sea turbidites: crustal evolution and plate tectonic associations. *Geochimica et Cosmochimica Acta*, 54, 2015–2050.
- Mongelli, G., Critelli, S., Perri, F., Sonnino, M., & Perrone, V. (2006). Sedimentary recycling, provenance and paleoweathering from chemistry and mineralogy of Mesozoic continental redbed mudrocks, Peloritani Mountains, Southern Italy. *Geochimical Journal*, 40, 197–209.
- Nagarajan, R., Armstrong-Altrin, J. S., Kessler, F. L., Hidalgo-Moral, E. L., Dodge Wan, D., & Taib, N. I. (2015). Provenance and tectonic setting of Miocene siliciclastic sediments, Sibuti Formation, northwestern Borneo. *Arabian Journal of Geosciences*, 8, 8549–8565.
- Nesbitt, H., & Young, G. (1982). Early Proterozoic climates and plate motions inferred from major element chemistry of lutites. *Nature*, 299, 715–717.
- Nesbitt, H. W., & Young, G. M. (1984). Prediction of some weathering trends of plutonic and volcanic rocks based on thermodynamic and kinetic considerations. *Geochimica et Cosmochimica Acta*, 48, 1523–1534.
- Nielsen, M. T., Weibel, R., & Friis, H. (2015). Provenance of gravity-flow sandstones from the Upper Jurassic-Lower Cretaceous Farsund Formation, Danish Central Graben, North Sea. *Marine and Petroleum Geology*, 59, 371–389.
- Offler, R., & Fergusson, C. L. (2016). Proto-Pacific-margin source for the Ordovician turbidite submarine fan, Lachlan orogen, southeast Australia: Geochemical constraints. *Sedimentary Geology*, 334, 53–65.
- Pantopoulos, G., & Zelilidis, A. (2012). Petrographic and geochemical characteristics of Paleogene turbidite deposits in the southern Aegean (Karpathos Island, SE Greece): Implications for provenance and tectonic setting. *Chemie der Erde – Geochemistry*, 72, 153–166.
- Prendergast, E., Offler, R., Phillips, D., & Zwingmann, H. (2011). $^{40}\text{Ar}/^{39}\text{Ar}$ and K-Ar ages: early Paleozoic metamorphism and deformation in the Narooma accretionary complex, NSW. *Australian Journal of Earth Sciences*, 58, 21–32.
- Purejav, N., & Roser, B. (2013). Geochemistry of Silurian-Carboniferous sedimentary rocks of the Ulaanbaatar terrane, Hangay-Hentey belt, central Mongolia: Provenance, paleoweathering, tectonic setting, and relationship with the neighbouring Tsetserleg terrane. *Chemie der Erde – Geochemistry*, 73, 481–493.
- R Core Team. (2020). *R: A language and environment for statistical computing*. Vienna, Austria: R Foundation for Statistical Computing <https://www.R-project.org/>.
- Rollinson, H. (1993). *Using geochemical data: Evaluation, presentation, interpretation*. Harlow, UK: Longman 352 p.
- Rosenbaum, G. (2018). The Tasmanides: Phanerozoic tectonic evolution of eastern Australia. *Annual Review of Earth and Planetary Sciences*, 46, 291–325.
- Roser, B. P., & Korsch, R. J. (1986). Determination of tectonic setting of sandstone-mudstone suites using SiO_2 content and $\text{K}_2\text{O}/\text{Na}_2\text{O}$ ratio. *Journal of Geology*, 94, 635–650.
- Rudnick, R. L., & Gao, S. (2003). Composition of the continental crust. In R. L. Rudnick (Ed.), *Treatise on Geochemistry. The Crust* (Vol. 3, pp. 1–64). Amsterdam: Elsevier.

- Runnegar, B. N. (1980). Biostratigraphy of the Shoalhaven Group. *N.S.W Geological Survey Bulletin*, Sydney, 26, 376–382.
- Ryan, K. M., & Williams, D. M. (2007). Testing the reliability of discrimination diagrams for determining the tectonic depositional environment of ancient sedimentary basins. *Chemical Geology*, 242, 103–125.
- Rygel, M. C., Fielding, R. C., Bann, L. K., Frank, T. D., Birgenheier, L., & Tye, C. S. (2008). The Lower Permian Wasp Head Formation, Sydney Basin: high-latitude, shallow marine sedimentation following the Late Asselian to Early Sakmarian glacial event in eastern Australia. *Sedimentology*, 55, 1517–1540.
- Shaanan, U., Rosenbaum, G., & Wormald, R. (2015). Provenance of the Early Permian Nambucca block (eastern Australia) and implications for the role of trench retreat in accretionary orogens. *Geological Society of America Bulletin*, 127, 1052–1063.
- Tao, H., Sun, S., Wang, Q., Yang, X., & Jiang, L. (2014). Petrography and geochemistry of Lower Carboniferous greywacke and mudstones in Northeast Junggar, China: Implications for provenance, source weathering, and tectonic setting. *Journal of Asian Earth Sciences*, 87, 11–25.
- Tawfik, H. A., Salah, M. K., Maejima, W., Armstrong-Altrin, J. S., Abdel-Hameed, A. T., & Ghadour, I. M. (2017). Petrography and geochemistry of the Lower Miocene Moghra sandstones, Qattara Depression, north Western Desert, Egypt. *Geological Journal*, 53, 1938–1953.
- Taylor, S. R., & McLennan, S. M. (1985). *The continental crust: Its composition and evolution*. Oxford, UK: Blackwell 1–349.
- Thomas, S. G., Fielding, C. R., & Frank, T. D. (2007). Lithostratigraphy of the late Early Permian (Kungurian) Wandrawandian Siltstone, New South Wales: Record of glaciation? *Australian Journal of Earth Sciences*, 54, 1057–1071.
- Tobia, F. H., & Shangola, S. S. (2016). Mineralogy, geochemistry, and depositional environment of the Beduh shale (lower Triassic), Northern Thrust Zone, Iraq. *Turkish Journal of Earth Sciences*, 25, 367–391.
- Tye, S. C., Fielding, C. R., & Jones, B. G. (1996). Stratigraphy and sedimentology of the Permian Talaterang and Shoalhaven Groups in the southernmost Sydney Basin, New South Wales. *Australian Journal of Earth Sciences*, 43, 57–69.
- Valloni, R., & Maynard, J. B. (1981). Detrital modes of recent deep-sea sands and their relation to tectonic settings: A first approximation. *Sedimentology*, 28, 75–83.
- Veevers, J. J. (2013). Pangea: Geochronological correlation of successive environmental and strati-tectonic phases in Europe and Australia. *Earth-Science Reviews*, 127, 48–95.
- Veevers, J. J., Belousova, E. A., Saeed, A., Sircombe, K., Cooper, A. F., & Read, S. E. (2006). Pan-Gondwanaland detrital zircons from Australia analysed for Hf-isotopes and trace elements reflect an ice-covered Antarctic provenance of 700–500 Ma age, TDM of 2.0–1.0 Ga, and alkaline affinity. *Earth-Science Reviews*, 76, 135–174.
- Veevers, J. J., Conaghan, P. J., & Powell, C. M. (1994). Eastern Australia. In J. J. Veevers & C. M. Powell (Eds.), *Permian-Triassic Pangean Basins and Foldbelts along the Panthalassan Margin of Gondwanaland* (Vol. 184, pp. 11–171). Colorado: Geological Society of America Bulletin.
- Verma, S. P., & Armstrong-Altrin, J. S. (2013). New multi-dimensional diagrams for tectonic discrimination of siliciclastic sediments and their application to Precambrian basins. *Chemical Geology*, 355, 117–133.
- Verma, S. P., & Armstrong-Altrin, J. S. (2016). Geochemical discrimination of siliciclastic sediments from active and passive margin settings. *Sedimentary Geology*, 332, 1–12.
- Verma, S. P., Pandarinath, K., Verma, S. K., & Agrawal, S. (2013). Fifteen new-discrimination function-based multidimensional robust diagrams for acid rocks and application to Precambrian rocks. *Lithos*, 168, 113–123.
- von Eynatten, H., Barceló-Vidal, C., & Pawlowsky-Glahn, V. (2003). Composition and discrimination of sandstones: a statistical evaluation of different analytical methods. *Journal of Sedimentary Research*, 73, 47–57.
- Young, G. M., & Nesbitt, H. W. (1999). Paleoclimatology and provenance of the glaciogenic Gowganda Formation (Paleoproterozoic), Ontario, Canada: A chemostratigraphic approach. *Geological Society of America Bulletin*, 111, 264–274.
- Zaid, S. M., & Gahtani, F. A. (2015). Provenance, diagenesis, tectonic setting and geochemistry of Hawkesbury sandstone (Middle Triassic), southern Sydney Basin, Australia. *Turkish Journal of Earth Sciences*, 24, 72–98.

SUPPORTING INFORMATION

Additional supporting information may be found online in the Supporting Information section at the end of this article.

How to cite this article: Maravelis AG, Offler R, Pantopoulos G, Collins WJ. Provenance and tectonic setting of the Early Permian sedimentary succession in the southern edge of the Sydney Basin, eastern Australia. *Geological Journal*. 2020;1–19. <https://doi.org/10.1002/gj.4051>